New perspectives of functional metal borohydrides

Jakob B. Grinderslev [a,1], Mads B. Amdisen [a,2], Lasse N. Skov [a,3], Kasper T. Møller [b,4], Lasse G. Kristensen [a,5], Marek Polanski [c,6], Michael Heere [d,e,7], Torben R. Jensen [a,*,8]

[a] Interdisciplinary Nanoscience Center (iNANO) and Department of Chemistry, University of Århus, Langelandsgade 140, DK-8000 Århus C, Denmark
[b] Department of Biological and Chemical Engineering, Aarhus University, Aabogade 40, 8200 Aarhus N, Denmark
[c] Department of Functional Materials and Hydrogen Technology, Military University of Technology, 00-908 Warsaw, Poland
[d] Institute for Applied Materials – Energy Storage Systems (IAM-ESS), Karlsruhe Institute of Technology (KIT), Hermann-von-Helmholtz-Platz 1, 76344 Eggenstein-Leopoldshafen, Germany
[e] Heinz Maier-Leibnitz Zentrum (MLZ), Technische Universität München, Lichtenbergstr. 1, Garching b, 85748 München, Germany

ARTICLE INFO

ABSTRACT

The chemistry of metal borohydrides and their derivatives has expanded signficantly during the past decade involving new compositions, structures, and the diversity of associated properties. Here we provide an overview of interesting results mainly from the past few years, discussed relative to previously published results. A range of new synthesis strategies has been developed to obtain pure samples, which has allowed very detailed structural, physical, and chemical investigations. A short overview of mono- and dimetallic borohydrides is provided, including a description of the complete series of rare-earth metal borohydrides and the recently discovered ammonium metal borohydrides, where the latter has attracted interest due to an extreme hydrogen content. Metal borohydrides appear to be the most promising class of materials to achieve high cationic conductivity of divalent metals, and particularly derivatives of metal borohydrides with neutral molecules show promise as future electrolytes for new types of solid-state batteries. Furthermore, metal borohydrides display a wide range of other properties, including optical, magnetic, semi conduction and possibly superconducting properties, and are also used as a new approach for carbon capture and conversion. The aim of the present review is to highlight new trends in properties and provide an outlook with possible future applications. Here, we focus on the more recently discovered materials.

1. Introduction

The extensive boron-hydrogen chemistry was developed in the 20th century. The smallest molecular member, BH_3, is also the least stable owing to electron deficiency and only exists as a gas molecule at extremely low partial pressures. This molecule has a stong tendency to dimerise to diborane, B_2H_6, with two bridging hydrogens shared by the two borons, and four remaining terminal hydrogens forming a slightly distorted tetrahedral coordination geometry of boron. Another type of addition reaction that can stabilize trihydromonoboran, BH_3, is the addition of a hydride ion, H^-, forming an anionic tetrahedral complex, tetrahydridoborate, BH_4^-, also known as the borohydride anion.

Since the first oil crisis in the 1970s, it has become increasingly clear that our consumption of fossil fuels must be terminated, in particular owing to increasing amounts of evidence for irreversible climatic changes. Although we already harvest renewable energy using windmills and solar cells, the implementation of 'green energy' is relatively slow [1]. This is due to the lack of a versatile energy storage medium for mobile and stationary applications. Hydrogen, suggested already in the 1970s, still appears as the most ideal option and can be transported in pipelines similar to natural gas. However, the low density, both as a gas and as a liquid, has been considered as a drawback, which has afforded significant focus on solid-state

* Corresponding author.
E-mail addresses: Jakobg@inano.au.dk (J.B. Grinderslev),
Mba@inano.au.dk (M.B. Amdisen), Lnskov@inano.au.dk (L.N. Skov),
ktm@bce.au.dk (K.T. Møller), marek.polanski@wat.edu.pl (M. Polanski),
michael.heere@kit.edu (M. Heere), trj@chem.au.dk (T.R. Jensen).
[1] orcid: 0000-0001-7645-1383.
[2] orcid : 0000-0003-2663-8988.
[3] orcid: 0000-0001-5427-2632.
[4] orcid: 0000-0002-1970-6703
[5] orcid: 0000-0001-9492-4690
[6] orcid: 0000-0003-0163-514X.
[7] orcid: 0000-0002-7826-1425.
[8] orcid: 0000-0002-4278-322.

Table 1

Properties of selected metal hydrides: molecular weight (M), material density (ρ), gravimetric hydrogen content (ρ_m), volumetric hydrogen density (ρ_v), and the onset of hydrogen release (T_{dec}). 'Reversibility' is also indicated with 'yes' in case hydrogen uptake takes place at moderate conditions. Notice that, $\rho_V = \rho_m \cdot \rho$.

	M (g mol^{-1})	ρ (g mL^{-1})	ρ_m (wt% H)	ρ_V (g H L^{-1})	Hydrogen storage		Ref.
					Reversibility	T_{dec}^{a} (°C)	
MgH_2	26.32	1.42	7.7	108.7	Yes	314[b]	[5]
Mg_2FeH_6	110.50	2.74	5.5	149.9	Yes	~350	[6–10]
Mg_2CoH_5	112.58	2.89	4.5	129.5	Yes	~320	[11–15]
Mg_2NiH_4	111.34	2.70	3.6	97.8	Yes	~300	[16]
$2LiBH_4$-MgH_2	69.88	0.84	14.4	120.4	Yes	~350–400	[17–19]
$LiBH_4$	21.78	0.67	18.5	124.0	No	~400	[18]
$NaBH_4$	37.83	1.07	10.7	114.4	No	~500	[20]
NH_4BH_4	32.88	0.69	24.5	157.0	No	~53	[21]
$(NH_4)_3Mg(BH_4)_5$	152.63	0.75	21.1	158.2	No	~37	[22]
$Mg(BH_4)_2 \cdot 2NH_3$	88.05	0.81	16.0	130.4	No	~120	[23]

[a] Decomposition temperatures strongly depend on the physical conditions for the measurement and the published data scatters significantly.
[b] at $p(H_2)$ = 2.3 bar.

hydrogen storage [2–4]. Hydrogen is usually packed more densely in the solid state as compared to that of the liquid, $\rho(H_{2\,(liq)})$ = 71 g H_2/L. This is illustrated by the high volumetric hydrogen densities of selected solid-state hydrogen storage compounds in Table 1.

Pre-millennium research focused on the reversible hydrogen storage in MgH_2 and complex hydride derivatives, such as Mg_2FeH_6, Mg_2CoH_5, and Mg_2NiH_4. These compounds are considered to store hydrogen reversibly because hydrogen release and uptake occur at moderate conditions, i.e. 300 < T < 450 °C at hydrogen pressures below 100 bar. However, the gravimetric hydrogen density is in some cases too low for practical applications.

In the early part of the 21st century, there was a significant interest in the chemistry of metal borohydrides, which has expanded this class of compounds beyond the early focus on alkali metal borohydrides and their applications. At present, metal borohydrides are known for all the alkali and alkaline earth metals and the entire range of the lanthanides (not including radioactive elements). Several metal borohydrides are also reported among the d-block elements and the actinides, but these are often less stable and challenging to isolate. Moreover, di- and trimetallic borohydrides readily form, which has resulted in a remarkable amount of new materials in the past decade [24–28].

Common to these is a high hydrogen content, in particular for the light-weight metals, and as such, these materials were particularly investigated for solid-state hydrogen storage. A range of synthetic strategies has provided pure, well-crystalline materials, which allowed very detailed investigations of the crystal structures and physical and chemical properties. Previously, in the late 1990's and early 2000s, the dominating synthesis method was mechano-chemically induced metathesis reactions, which often results in a multi-phase sample hampering detailed investigations. But in the past decade, new synthesis strategies have allowed for synthesis of more pure and new metal borohydrides, which cannot be obtained by the mechano-chemical approach.

The ideal solid-state hydrogen storage material is ammonium borohydride, NH_4BH_4, which is isoelectronic to natural gas, CH_4. This compound has an extremely high gravimetric (ρ_m = 24.5 wt% H) and volumetric (ρ_V = 157.0 g H/L) hydrogen density, which is the highest values among the known inorganic materials [29]. Unfortunately, ammonium borohydride is only metastable at room temperature with a half-life of ~6 h and spontaneously decomposes to the diammoniate of diborane, and also releases hydrogen and toxic gases such as borazine and ammonia during further decomposition [21,30,31]. Systematic studies of addition reactions between ammonium borohydride, NH_4BH_4, and metal borohydrides, $M(BH_4)_n$, revealed a multitude of novel ammonium metal borohydrides and ammonium metal borohydride derivatives [22,32,33]. These compounds also exhibit extremely high hydrogen densities as shown in

Fig. 1. However, unwanted gases are often released during decomposition. High hydrogen density compounds are also formed from ammine metal borohydrides, but reversibility and NH_3 versus H_2 release is a major issue for hydrogen storage applications [34–36].

In general, metal borohydrides suffer from poor thermodynamics (large numerical value of enthalpy change for hydrogen release and uptake) and slow kinetics during rehydrogenation, making them unsuitable for hydrogen storage. However, two or more hydrides may react during the release of hydrogen, forming a so-called *reactive hydride composite* (RHC), where a new dehydrogenated state is formed [37]. The hydrogen storage densities of RHC systems is the average of the components, but they may have significantly improved thermodynamic and kinetic properties, which can facilitate reversible hydrogen release and uptake. The enthalpy change for hydrogen release for the individual components, $LiBH_4$ and MgH_2, is ΔH_{dec} = 68.9 and 74.1 kJ/mol, respectively [5,38,39]. However, the endothermic dehydrogenation of the $2LiBH_4$–MgH_2 composite also includes an exothermic formation of MgB_2, which lowers the total reaction enthalpy to ΔH_{dec} ~ 46 kJ/mol. The hydrogen release temperature corresponding to this calculated decomposition enthalpy assuming $p(H_2)$ = 1 bar is T ~ 169 °C [17,40]. Then, the hydrogen absorption proceeds from the MgB_2–LiH composite but at somewhat higher temperatures due to kinetic restraints, $p(H_2)$ = 50 bar and T < 300 °C, which is a significant improvement as compared to rehydrogenation of the individual components.

Today, other options for hydrogen storage are also considered, such as extraction of carbon dioxide from air or biomass, which can be reacted with hydrogen to form methanol, resulting in a 'carbon-neutral' fuel [41,42]. Another option is the direct reaction of a metal borohydride with CO_2 to form formic acid. At low partial pressures of CO_2, only one molecule is absorbed, but at more ideal conditions, three molecules react with one borohydride anion to form a tri-formatoborohydride anion, $[HB(OCHO)_3]^-$ [43].

While metal borohydrides and their derivatives appear challenging to use for reversible hydrogen storage, a large number of other interesting properties have been discovered in the past decade, relevant for applications as solid-state electrolytes [44–51], magnetic materials [26,52–54], luminescent materials [54–57], gas-adsorption [58,59], polymerization initiators [60–64], and explosives [65]. Their use as electrolytes for all-solid-state batteries has received particular interest, and several physical phenomena which can enhance the ionic conductivity have been proposed for this class of materials. The *paddle-wheel* mechanism for cationic conductivity is related to the dynamics of the anions, which upon reorientations facilitate the migration of the cations [66]. This effect has been observed in some metal borohydrides, e.g. it was found that the cation jump rate is on the same frequency scale as the BH_4^- dynamics in $LiLa(BH_4)_3X$ (X = Cl, Br, I) [67–69]. More recently, it was found that a neutral molecule
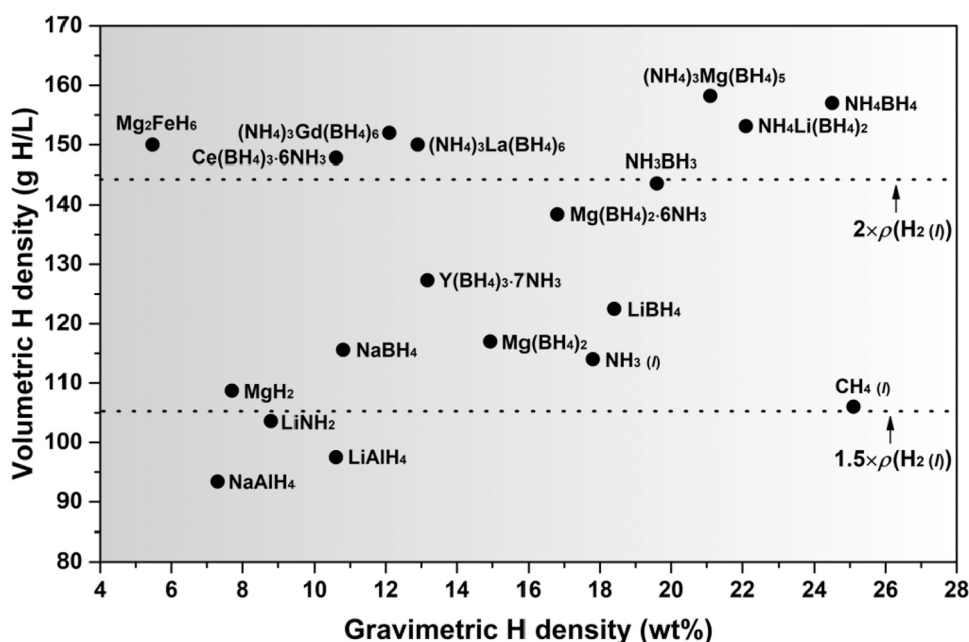
Fig. 1. Gravimetric and volumetric H content of selected metal hydrides.

can significantly enhance the ionic conductivity, applicable to both monovalent and divalent metals [49–51,70–73]. A new cation conductivity mechanism has been suggested, which is discussed in more detail in Chapter 4.

Thus, metal borohydrides and their derivatives have expanded extremely fast during the past decade regarding new compositions, structures and also in the diversity of associated properties. The aim of the present review is to highlight new trends in properties and provide an outlook with possible future applications. The multitude of recent results justifies the present review, which will give the reader an overview of the recent advances, which are discussed in a larger perspective relative to the previously published literature.

2. Synthesis of $M(BH_4)_n$ compounds and their derivatives

Already in 1940, the first homoleptic metal borohydrides, i.e. $LiBH_4$, $Be(BH_4)_2$, and $Al(BH_4)_3$, were reported. The synthesis approach utilised the reaction between metal alkyls and gaseous diborane, B_2H_6 [74–76]. The synthesis approach was later expanded to include the reaction of a metal hydride or alkoxide with B_2H_6 to produce the metal borohydride [77–79]. However, the poisonous B_2H_6 gas as a reactant is preferably avoided also due to possible self-ignition in contact with air.

Commercially, $NaBH_4$ is widely used in organic chemistry as a reducing agent [80,81], and the synthesis of the compound follows the Brown-Schlesinger method reacting sodium hydride with trimethylborate: [82].

$$4\ NaH + B(OCH_3)_3 \rightarrow NaBH_4 + 3\ NaOCH_3 \tag{1}$$
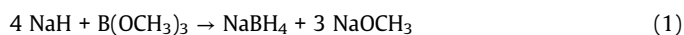
At present, the main methods for synthesis of new metal borohydrides are mechanochemical- or solvent-mediated synthesis methods as discussed in the following.

### 2.1. Mechanochemical synthesis of $M(BH_4)_n$ compounds

Mechano-chemistry has been widely utilised to synthesize metal borohydrides, and new compounds have often been discovered through a metathesis reaction between, typically, $LiBH_4$ or $NaBH_4$, and a metal halide, MX_n, which often yields the monometallic borohydride and the lithium or sodium halide salt, see example in reaction scheme 2 [83–90].

$$n\ LiBH_4 + MX_n \rightarrow n\ LiX + M(BH_4)_n \tag{2}$$
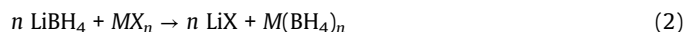
When utilising $LiBH_4$ or $NaBH_4$ as the precursor, monometallic borohydrides are obtained, likely due to the high stability of the formed LiCl and NaCl salt, whereas the heavier alkali metal borohydrides, MBH_4 (M = K, Rb, Cs), often lead to dimetallic borohydrides [24,25]. However, the mechano-chemical approach may also result in a reaction between the metal halide and the metal borohydride forming solid solutions or mixed metal borohydride-halide compounds [24,25,45,91–94]. A variety of compounds are prepared when rare-earth metal (RE) halides ($RECl_3$) are ball milled with $LiBH_4$, which leads to $LiRE(BH_4)_3Cl$, $LiRE(BH_4)_4$, α-$RE(BH_4)_3$, β-$RE(BH_4)_3$ or $RE(BH_4)_2$, dependent on the RE-ion and the synthesis conditions [88,91,92,95–97]. To obtain a pure sample, solvent extraction may be an option [22,24,89,90,98–101], although by-products, e.g. dimetallic borohydrides or unreacted $LiBH_4$ may be soluble in the selected solvent and thus hampers this method [99,102–104]. Thus, the choice of solvent is crucial to obtain a pure sample.

When utilising pristine monometallic borohydrides, an addition reaction may occur during mechano-chemistry, which is observed, e.g. for MBH_4 (M = K, Rb, Cs), and strontium or samarium borohydride (see reaction scheme 3) [105,106].

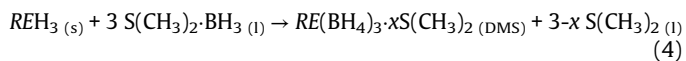$$MBH_4\ _{(s)} + Sr(BH_4)_2\ _{(s)} \rightarrow MSr(BH_4)_3\ _{(s)} \tag{3}$$
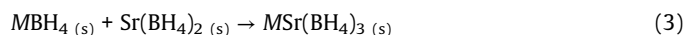
Finally, thermal treatment at 200 °C and subsequent quenching has been demonstrated to provide dimetallic compounds based on Y($BH_4)_3$, i.e. $MY(BH_4)_4$ (M = Li, Na) [107].
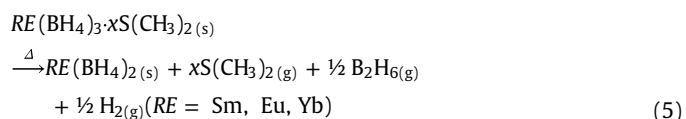
2.2. Solvent-mediated synthesis of $M(BH_4)_n$ compounds

Over the years, solvent-mediated synthesis of metal borohydrides has been developed using borane donor complexes, i.e. tetrahydrofuran borane ($THF\cdot BH_3$) [105], trimethylamine borane ($TEA\cdot BH_3$) [108–110], and dimethyl sulfide borane ($DMS\cdot BH_3$) [26,106,111,112]. An example is $Mg(BH_4)_2$, which is synthesized from di-n-butylmagnesium ($Mg(Bu)_2$) and $DMS\cdot BH_3$, through the

precipitation of $Mg(BH_4)_2 \cdot \frac{1}{2}S(CH_3)_2$. Hence, unreacted starting materials are removed by simple filtration, while the solvent-free metal borohydride can be obtained upon thermal treatment [112]. Thus, the major advantage of the synthesis method is that pure metal borohydrides are produced with a high selectivity of the polymorphs [26,111].

The method was later successfully applied to the reaction between metal hydrides and the borane donor complexes [111], e.g. the entire series of $RE(BH_4)_x$ ($x = 2$ or 3) was produced: [26].

$$RE H_{3 \ (s)} + 3 \ S(CH_3)_2 \cdot BH_{3 \ (l)} \rightarrow RE(BH_4)_3 \cdot xS(CH_3)_{2 \ (DMS)} + 3 - x \ S(CH_3)_{2 \ (l)} \tag{4}$$
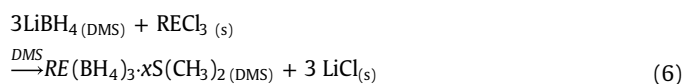
However, the method is limited to ionic or covalent metal hydrides, as metallic hydrides do not react with the borane donor complex. This was observed by the difference in reactivity of SmH_2/SmH_3 and CeH_2/CeH_3, of which only the REH_3 compounds are ionic and react with $DMS \cdot BH_3$ to form $RE(BH_4)_3 \cdot xS(CH_3)_2$ [26,111]. Removal of DMS upon heating usually results in the metal borohydride, but in the case of $RE(BH_4)_3 \cdot xS(CH_3)_2$ (RE^{3+} = Sm, Eu, Yb), a reduction from RE^{3+} to RE^{2+} occurs due to the stable +II oxidation state:

$$RE(BH_4)_3 \cdot xS(CH_3)_{2 \ (s)}$$
$$\xrightarrow{\Delta} RE(BH_4)_{2 \ (s)} + xS(CH_3)_{2 \ (g)} + \frac{1}{2} \ B_2H_{6(g)}$$
$$+ \frac{1}{2} \ H_{2(g)} (RE = \ Sm, \ Eu, \ Yb) \tag{5}$$

The use of solvent-mediated synthesis has the advantages of (*i*) faster reaction kinetics as the product is dissolved in the solvent, i.e. the equilibrium is shifted towards the product (*ii*) pure compounds are easily obtained if weakly coordinating solvents are utilized (*iii*) the undesired metal halides have a low solubility in the solvents and are thus omitted in the product. The coordination strength of the solvents depends on the electron-donating element and typically increases in the order of S < N < O, thus DMS is the preferred solvent as it is the easiest to remove by thermal treatment, which allows a higher polymorphic selectivity of the reaction product [24,111].

Simple metathesis reactions have also been observed in solvent-mediated reactions between $LiBH_4$ and the series of $RECl_3$ (RE = La, Ce, Pr, Sm, Eu, Gd, Dy, Er) in DMS as shown in reaction scheme (6).

$$3LiBH_{4 \ (DMS)} + RECl_{3 \ (s)}$$
$$\xrightarrow{DMS} RE(BH_4)_3 \cdot xS(CH_3)_{2 \ (DMS)} + 3 \ LiCl_{(s)} \tag{6}$$

The drawback is the solubility of $LiBH_4$ in DMS, which, in case of incomplete reaction, results in the presence of $LiBH_4$ in the product [104]. However, the presence of $LiBH_4$ can be suppressed by using an excess of the $RECl_3$.

Finally, it is possible to form dimetallic borohydrides directly from solvent-mediated synthesis, which was demonstrated for $LiZn_2(BH_4)_5$ and $MY(BH_4)_4$ (M = Li, Na, K, Rb, Cs) [113,114]. Thus, the procedure opened up new avenues for synthesizing new dimetallic borohydrides as $MY(BH_4)_4$ (M = Li, Na) was not obtainable by mechano-chemistry owing to the metastable nature of the compounds at room temperature [113].

2.3. Synthesis of metal borohydride derivatives

Ammine metal borohydrides may be synthesised by the metathesis reaction between an ammine metal chloride and lithium borohydride through the classic mechano-chemistry approach as observed for the reaction between lithium borohydride and titanium chloride (see reaction scheme 7) [115–118].

$$3 \ LiBH_4 + TiCl_3 \cdot xNH_3 \rightarrow 3 \ LiCl + Ti(BH_4)_3 \cdot xNH_3 \ (x = 3 \ or \ 5) \tag{7}$$
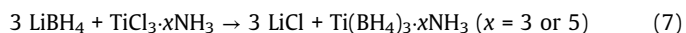
The procedure described in Section 2.2 has allowed the synthesis of pure metal borohydrides, which subsequently may be utilized to

synthesize pure ammine metal borohydrides [26,111,119]. Hence, a direct reaction may proceed between the pristine metal borohydride and liquid or gaseous ammonia [24], or alternatively via ligand exchange in solution, see reaction scheme 8 [101,119,120].

$$M(BH_4)_n + x \ NH_3 \rightarrow M(BH_4)_n \cdot xNH_3 \tag{8}$$
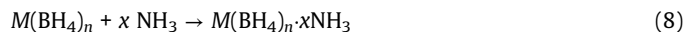
The latter method has also been applied to the unstable transition metal borohydrides, e.g. Ti^{3+} (d^1), V^{3+} (d^2), Fe^{2+} (d^6), and Co^{2+} (d^7), as the coordination of NH_3 provides a stabilizing effect, allowing the compounds to be investigated at room temperature [115,120,121]. Interestingly, compounds such as the bicationic $(NH_4)_nM(BH_4)_m \cdot xNH_3$ compounds are produced through the decomposition of $(NH_4)_{n+1}M(BH_4)_{m+1}$ as they release H_2 and B_2H_6 [22].

3. Structural diversity of metal borohydrides

Metal borohydrides exhibit an extreme structural flexibility related to the diverse coordination of the BH_4^- anion, which can coordinate to a metal as a corner- ($B-H$, κ^1), edge- ($B-H_2$, κ^2), or face-sharing ($B-H_3$, κ^3) ligand, and it can act as a counter ion. The structures of most metal borohydrides are described in ref [24,25] and the following sections will focus on selected cases and recently discovered metal borohydrides.

The structures of most monometallic borohydrides consist of three-dimensional frameworks of $[M(BH_4)_4]$ tetrahedra or $[M(BH_4)_6]$ octahedra, where BH_4^- acts as bridging ligand, often by edge-sharing of the BH_4-tetrahedron (κ^2) [24,25]. This is highlighted by the examples of $Mg(BH_4)_2$ and $RE(BH_4)_3$ described in subsection 3.1 and 3.2, respectively. There are also few examples of molecular monometallic borohydrides, $Al(BH_4)_3$, $Ti(BH_4)_3$, $Zr(BH_4)_4$, and $Hf(BH_4)_4$, which are volatile or gases at room temperature, due to the lack of an interconnecting network [122–125]. Monometallic borohydrides often exhibit polymorphism, and particularly $Mg(BH_4)_2$ has attracted significant interest from a structural point of view since this composition exists in the highest number of different polymorphs, including a permanent nano-porous and amorphous state.

3.1. Polymorphism of magnesium borohydride

With five structurally identified and two yet unsolved compounds of magnesium borohydride, the structures of α-, β-, γ-, δ-, ζ- and β'-, ε- $Mg(BH_4)_2$, respectively, display the most diverse polymorphism among metal borohydrides, see Fig. 2 [126,127]. All the known polymorphs consist of tetrahedral $[Mg(BH_4)_4]$ complexes, where each BH_4^- is bridging two Mg^{2+}. Interestingly, the topology of each polymorph is different as highlighted by the polyhedra in the figure, where all $[Mg(BH_4)_4]$ tetrahedra are connected in three-dimensional frameworks in α-, β-, γ- and ζ-$Mg(BH_4)_2$, while δ-$Mg(BH_4)_2$ consists of two interpenetrating frameworks.

In addition to the crystalline polymorphs, $Mg(BH_4)_2$ can form an amorphous state, which can be obtained by different methods, including *i*) reactive ball milling of MgB_2 and H_2 [128] *ii*) ball milling of γ-$Mg(BH_4)_2$ [59] and *iii*) by a pressure collapse of γ-$Mg(BH_4)_2$ [129]. Upon heating the amorphous phase to above 90 °C, γ-$Mg(BH_4)_2$ can be reformed [129]. The high-pressure polymorph δ-$Mg(BH_4)_2$ can be formed at pressures above 1.1–2.1 GPa, but is stable upon decompression [59]. This polymorph has received special attention as it has one of the highest volumetric hydrogen capacities of all complex metal hydrides with 147 g H L^{-1}, considerably higher than the capacities for the other polymorphs, 82–117 g H L^{-1}.

The structure of γ-$Mg(BH_4)_2$ is built as a three-dimensional structure with interpenetrating channels, with an inner and outer diameter of ~8 and ~12.3 Å, respectively. Thus, the structure may be described as a metal organic framework-like structure with a porosity of ~33%, which can adsorb neutral guest molecules or noble gas
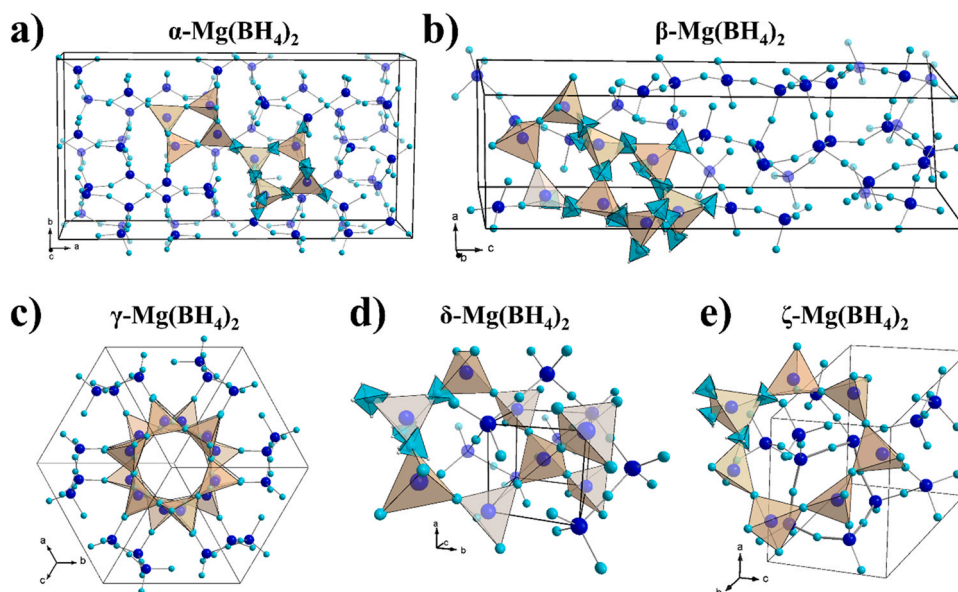
Fig. 2. Crystal structures of a) α-Mg(BH$_4$)$_2$ (*P6$_1$22*), b) β-Mg(BH$_4$)$_2$ (*Fddd*), c) γ-Mg(BH$_4$)$_2$ (*Ia-3d*), d) δ-Mg(BH$_4$)$_2$ (*P4$_2$nm*) and ζ-Mg(BH$_4$)$_2$ (*P3$_1$12*). Color scheme: Mg^{2+} (blue), B (light blue), H (grey). (For interpretation of the references to colour in this figure, the reader is referred to the web version of this article.)

atoms [59,130]. As an example, it was reported that up to 3 wt% of hydrogen can be adsorbed at − 193 °C and p(H$_2$) = 105 bar.

For the amorphous Mg(BH$_4$)$_2$, total X-ray scattering was recently combined with pair distribution function (PDF) analysis. It was suggested that the local ordering still bears a striking resemblance to the γ-polymorph, but only up to 5.1 Å, which is the length of the Mg−BH$_4$−Mg building blocks [131]. Another visible barrier is the outer diameter of the interpenetrating channels, where the data up to 12.3 Å suggested that those channels still existed [59,126]. Outside of those channels (r > 12.3 Å) the PDF became featureless, agreeing with the completely randomized structure [131].

Interestingly, the chemical reactivity of amorphous Mg(BH$_4$)$_2$ is different as compared to the crystalline forms, e.g. observed in the reaction with NH$_3$BH$_3$, where no reaction is observed for amorphous Mg(BH$_4$)$_2$, while the reaction with α-Mg(BH$_4$)$_2$ results in Mg (BH$_4$)$_2$·2NH$_3$BH$_3$ [132]. A mixture is obtained when using γ-Mg (BH$_4$)$_2$, due to the competing reactions to form amorphous Mg(BH$_4$)$_2$ and Mg(BH$_4$)$_2$·2NH$_3$BH$_3$ [132]. A similar difference was observed in the reactivity of α- and γ-Mg(BH$_4$)$_2$ with NH$_4$BH$_4$ [22]. Thus, the γ-polymorph should be avoided for subsequent synthesis involving ball milling, which has been used as a possible approach to tune the ligand content, e.g. the amount of NH$_3$ in Mg(BH$_4$)$_2$·xNH$_3$ [49,51,133], as this may result in the wrong composition of the obtained products.

3.2. Crystal structures of the rare-earth metal borohydrides

In recent years, rare-earth metal borohydrides (RE(BH$_4$)$_n$) have been investigated with different motivation, such as materials for solid-state hydrogen storage [4134] or as solid-state ionic conductors for battery applications [135,136] and reviewed in Refs [26,96,137]. The majority of the rare-earths form trivalent RE(BH$_4$)$_3$, but divalent RE(BH$_4$)$_2$ is formed for RE^{2+} = Sm, Eu, Yb due to a stable +II oxidation state. The structures of the divalent RE(BH$_4$)$_2$ are isostructural to the alkaline earth metal borohydrides with similar ionic radii, i.e. M (BH$_4$)$_2$ (M^{2+} = Sr) for RE^{2+} = Sm and Eu and M^{2+} = Ca for RE^{2+} = Yb [26,90,92,96,111].

The trivalent RE(BH$_4$)$_3$ can crystallize in three different structures, α- (*Pa-3*), β- (*Fm-3m*), and r-RE(BH$_4$)$_3$ (*R-3c*), all of them related to the cubic polymorphs of rhenium trioxide (ReO$_3$). In these structures, the RE atoms are octahedrally coordinated to six BH$_4^-$, where all the BH$_4^-$ groups are bridging the RE^{3+} centers. The crystal structures are shown in Fig. 3. β-RE(BH$_4$)$_3$ is the ideal ReO$_3$ structure, while α- and r-RE(BH$_4$)$_3$ may be obtained by tilting of the octahedra.

At room temperature, the larger rare-earths RE^{3+} = La and Ce crystallize in the r-RE(BH$_4$)$_3$ structure, while RE^{3+} = Ce can also crystallize in the α-RE(BH$_4$)$_3$ structure (Fig. 3). For the smaller RE^{3+} = Pr-Lu, the compounds crystallize in either the α- or β-RE(BH$_4$)$_3$, depending on the synthesis conditions [26,95]. The volume correlates linearly with the volume of the RE-ion, and it is evident that the volume increases in the order r-< α-< β-RE(BH$_4$)$_3$, resulting in a larger void space in β-RE(BH$_4$)$_3$.

The intermediate-sized RE(BH$_4$)$_3$ (RE^{3+} = Ce and Pr) are the only compounds showing all three polymorphs, i.e. α-, β- and r-RE(BH$_4$)$_3$ [26,98,137]. Upon heating, α-Ce(BH$_4$)$_3$ undergoes a polymorphic transition at ~129 °C into r-Ce(BH$_4$)$_3$, and a similar transition from β- to r-Ce(BH$_4$)$_3$ occurs at T > 175 °C [26,98]. This transition is not reversible upon cooling. In the case of Pr(BH$_4$)$_3$, the α-polymorph is stable at room temperature, and upon heating the structure changes to β-Pr(BH$_4$)$_3$ at ~190 °C, but this polymorph immediately transforms to r-Pr(BH$_4$)$_3$. This transformation is assigned to the large voids in the β-polymorph, which allow for bending of the Pr−BH$_4$−Pr bonds based on the rotation of Pr(BH$_4$)$_6$ octahedra, resulting in a more dense packing and transition to r-Pr(BH$_4$)$_3$ [137]. The transition from α- to r-Pr(BH$_4$)$_3$ is reversible under the right conditions [137], but a recent study did not reproduce the reversible transition nor the stepwise negative thermal expansion observed in ref [137,138]. The polymorphic transitions were also investigated under elevated hydrogen pressure (p(H$_2$) = 40 bar), resulting in the porous β-Pr(BH$_4$)$_3$ as the major phase at 190 °C, demonstrating that the polymorphic transitions are pressure dependent [137].

3.3. Di-metallic borohydrides

Dimetallic borohydrides are observed for several mixtures of alkali metal and alkaline earth metal or d- or f-block metal borohydrides. The majority of dimetallic borohydrides consist of complex anions, charge-balanced by the less electronegative alkali metal ion. Due to the difference in Pauling electronegativity, the more electronegative metal ion forms the center of the complex anion and
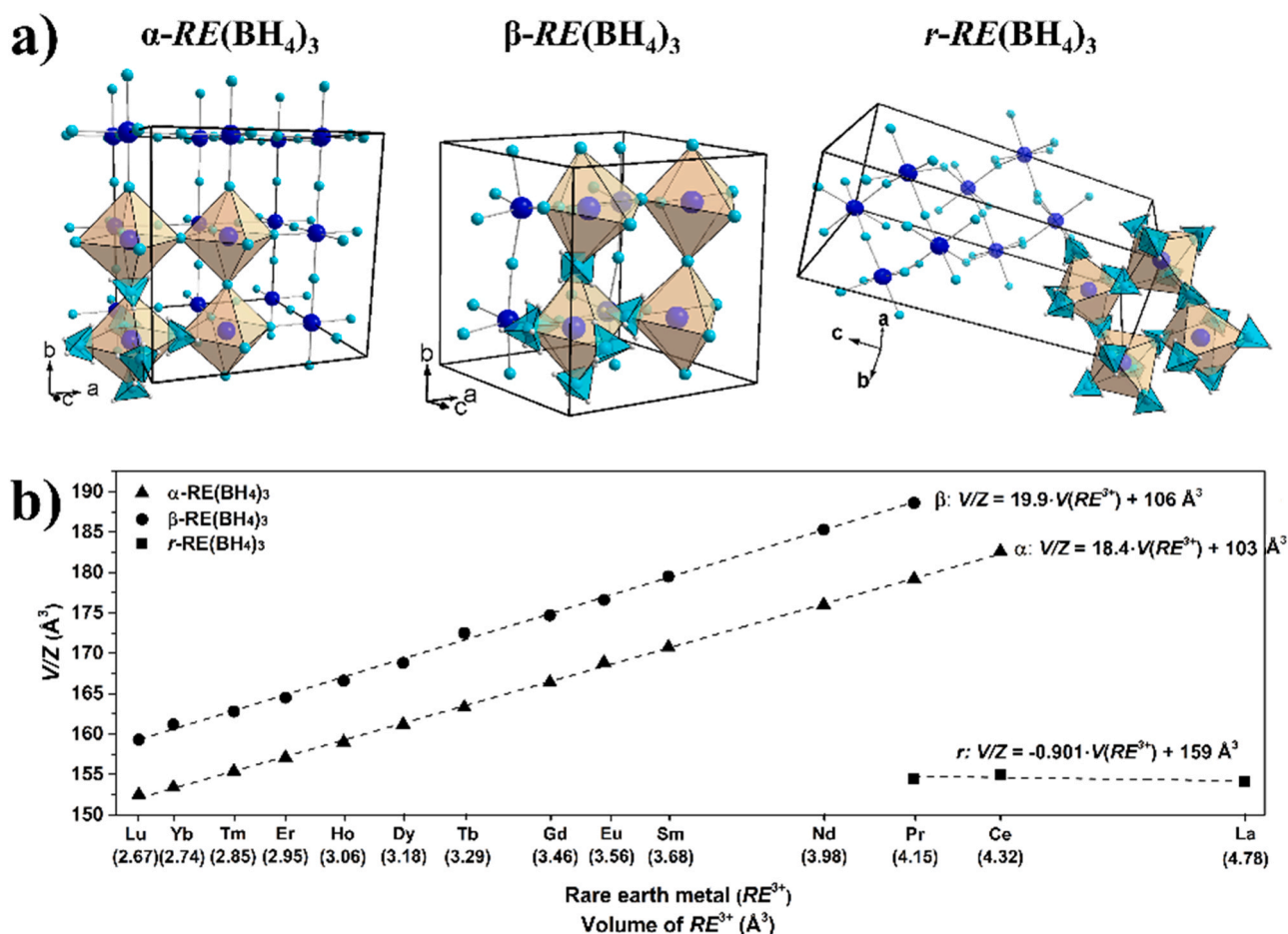
Fig. 3. a) Crystal structures of α-$RE(BH_4)_3$ (*Pa-3*), β-$RE(BH_4)_3$ (*Fm-3m*), and r-$RE(BH_4)_3$ (*R-3c*). Color scheme: RE^{3+} (blue), B (light blue), H (grey). b) Volume per formula unit (*V/Z*) of $RE(BH_4)_3$ as a function of the volume of the *RE*-ion ($V(RE^{3+})$) at room temperature. *V/Z* data are obtained from ref [26,88,95,138]. and the ionic radii are from ref [139]. (For interpretation of the references to colour in this figure, the reader is referred to the web version of this article.)

forms a more covalent bond to BH_4^-, while the bonding between the alkali metal and the BH_4^- is more ionic [22,24,25].

The anion complexes often exist as isolated anions, e.g. K_xMg $(BH_4)_{2+x}$ ($x = 2$, 3), where the structure is built from isolated [Mg $(BH_4)_4$]$^{2-}$ tetrahedra, which are charge balanced by K^+. In K_3Mg $(BH_4)_5$, one BH_4^- group also acts as a counter-anion [140]. Alkali metal calcium, strontium and samarium borohydrides form perovskite-type structures with the composition $M_1M_2(BH_4)_3$ (M_1 = K, Rb, Cs; M_2 = Ca, Sr, Sm), where the octahedrally coordinated M_2 are interconnected in three-dimensional frameworks via bridging κ^2-BH_4. These frameworks are charge-balanced by M_1 sitting in a cuboctahedral geometry consisting of twelve BH_4^- groups [55,105,106]. The crystal symmetry of the strontium perovskites increases upon heating, but are lower than the Ca-analogous at room temperature, suggesting that Sr^{2+} is too large to stabilize the ideal cubic perovskite structure [24]. Structurally, the borohydride-based perovskites differ from oxide and halide analogues due to dihydrogen repulsions between the BH_4^- ligands, which can result in a symmetry lowering during heating [55,141].

Recently, a large variety of new bi-cationic borohydrides was investigated, namely ammonium metal borohydrides, $(NH_4)_xM$ $(BH_4)_y$. Mixtures between NH_4BH_4 and $M(BH_4)_n$ have been investigated for M = Li, Na, K, Mg, Ca, Sr, Al, Sc, Y, Mn, La, Gd, forming new compounds with high hydrogen densities of 9.2–24.5 wt% H. No reaction was observed with $NaBH_4$, while a solid-solution was formed with KBH_4. This class of compounds displays a fascinating structural diversity, forming structures built from isolated tetrahedral, five-fold or octahedral anionic [$M(BH_4)_n$] complexes, to structures built from one-dimensional chain-like frameworks, two-dimensional layers to three-dimensional framework structures (Fig. 4). Many of the ammonium metal borohydrides show resemblance to the K- and Rb-analogues due to the similar ionic radii, *r* (NH_4^+) = 1.48 Å, $r(K^+)$ = 1.38 Å, and $r(Rb^+)$ = 1.52 Å, and thus the NH_4^+ is considered as a counter ion, similar to the alkali metals in dimetallic borohydrides [22].

Dihydrogen interactions between complex NH_4^+ and BH_4^- ions may contribute to a higher structural diversity and flexibility. This may be the reason for the formation of $(NH_4)_3La_2(BH_4)_9$, which has a new composition and structure type as compared to the alkali metal analogues. Furthermore, it was found that the shortest dihydrogen bonds, N-H$^{\delta+}\cdots^{-\delta}$H-B, in the structures, correlate with the structural dimensionality. The three-dimensional framework structures display significantly longer dihydrogen bonds compared to the structures with a lower dimensionality [22].

3.4. Metal borohydrides with neutral ligands

The compositional and structural diversity of metal borohydrides can be further expanded by the introduction of neutral ligands, which may alter the chemical and physical properties. These ligands often contain an atom with a free electron pair, e.g. N, O, or S, which can form a covalent bond to the metal-ion in the structure. This has resulted in a large range of solvated metal borohydrides, including ligands such as dimethyl sulphide, tetrahydrofuran, and a range of
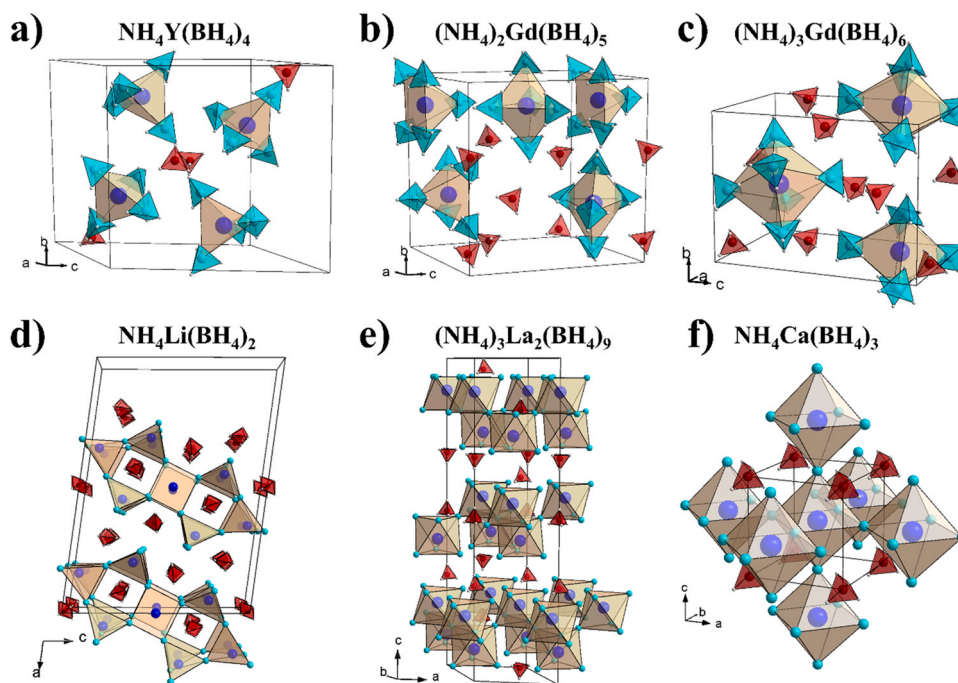
Fig. 4. Crystal structures of a) $NH_4Y(BH_4)_4$, b) $(NH_4)_2Gd(BH_4)_5$, c) $(NH_4)_3Gd(BH_4)_6$, d) $NH_4Li(BH_4)_2$, e) $(NH_4)_3La_2(BH_4)_9$, and f) $NH_4Ca(BH_4)_3$. The structures are built from isolated complex anions (a-c), one-dimensional chains (d), two-dimensional layers (e), and three-dimensional frameworks (f). Color scheme: M (blue), B (light blue), H (grey), BH_4^- (light blue tetrahedra), NH_4^+ (red tetrahedra). (For interpretation of the references to colour in this figure, the reader is referred to the web version of this article.)

different N-based ligands, e.g. NH_3, NH_3BH_3, and N_2H_4 [24,26,34,57,89,98,111,142,143]. The hydrogen atoms on the neutral ligands are often bonded to more electronegative atoms, e.g. C, N, O, or S, which results in dihydrogen interactions in the solid state, e.g. $B–H^{\delta-}\cdots^{+\delta}H–N$. Multiple compounds are known with strong dihydrogen interactions (< 2.4 Å), which stabilizes the structural framework, e.g. $Mg(BH_4)_2\cdot2NH_3BH_3$, $Sr(BH_4)_2\cdot2NH_3BH_3$, and $Al(BH_4)_3\cdot NH_3BH_3$ [132,144,145].

The most extensively studied class of metal borohydrides with neutral ligands is the ammines, which has been reported for almost all of the known metal borohydrides. This class of compounds display a large range of compositions, e.g. $Y(BH_4)_3\cdot xNH_3$, $x = 1$, α-2, β-2, α-3, β-3, 5, 6, 7. Ammine yttrium borohydrides is the only series showing polymorphism ($x = 2$ and 3), and $x = 3$, 5, 6, and 7 are isostructural with several members of the rare-earths [100,101,119,146]. Note that the structures of $Y(BH_4)_3\cdot xNH_3$ ($x = 3$, 5) have recently been revised [101,119,146]. The entire range of ammine rare-earth metal borohydrides was recently investigated, revealing interesting trends in compositions, crystal structures, and thermal properties [119]. It was found that the thermal stability correlated with the volume of the RE^{3+} ion, where the stability of $RE(BH_4)_3\cdot xNH_3$ ($x = 3$, 5, 7) increased with increasing cation charge-density, while $x = 4$ and α-6 decreased due to a too large coordination sphere to be accommodated by the decreasing volume of RE^{3+} [119].

The introduction of ammonia into the structures of metal borohydrides breaks down the three-dimensional frameworks, and the structural dimensionality usually decreases with increasing NH_3 content [100,101,119]. There are only few examples of ammine metal borohydrides with a three-dimensional framework structure, e.g. $M(BH_4)_2\cdot NH_3$ ($M^{2+} =$ Ca, Ba, Yb) and the bi-cationic $M_1M_2(BH_4)_3\cdot2NH_3$ ($M_1^+ =$ Li, NH_4; $M_2^{2+} =$ Mg, Mn) [22,35,119,147,148]. Compounds with low NH_3 content usually show two-dimensional layered or one-dimensional chain-like structures, while compounds with intermediate NH_3 content usually form neutral molecular compounds. The compounds with high NH_3 content usually form ionic complexes, where the metal cation is often fully coordinated by NH_3,

while the BH_4^- acts as a counter ion. However, there are few examples where BH_4^- can act as both a coordinating ligand and a counter ion in the same compound, e.g. α-$RE(BH_4)_3\cdot6NH_3$ ($RE^{3+} =$ La, Ce, Pr, Nd) and $RE(BH_4)_3\cdot5NH_3$ ($RE^{3+} =$ Y, La, Ce, Pr, Nd, Gd, Tb, Dy, Ho, Er, Tm, Yb). The trends in crystal chemistry are well illustrated by $Mg(BH_4)_2\cdot xNH_3$ ($x = 1$, 2, 3, 6), see Fig. 5, forming one-dimensional zig-zag chains for $x = 1$, neutral molecular $[Mg(BH_4)_2(NH_3)_x]$ complexes for $x = 2$ and 3, and ionic $[Mg(NH_3)_6]^{2+}$ and $[BH_4]^-$ complexes for $x = 6$ [23,36,49].
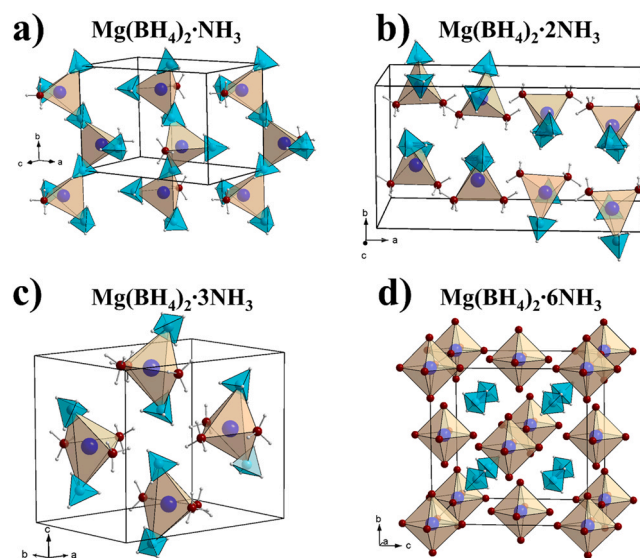
Fig. 5. Crystal structures of a) $Mg(BH_4)_2\cdot NH_3$, b) $Mg(BH_4)_2\cdot2NH_3$, c) $Mg(BH_4)_2\cdot3NH_3$, and d) $Mg(BH_4)_2\cdot6NH_3$. Color scheme: Mg^{2+} (blue), B (light blue), N (red), H (grey). (For interpretation of the references to colour in this figure, the reader is referred to the web version of this article.)

Ammonia always coordinates to the metal-ion via the lone pair on N, while BH_4^- displays a more flexible coordination. The BH_4^- group may act as a bridging or terminal ligand, often via edge-sharing (κ^2) or face-sharing (κ^3), respectively. However, the coordination of the BH_4^- usually orients in a way to satisfy the preferred coordination (including H) of the metal, which is typically ~8 for smaller cations such as Li^+ and Mg^{2+}, and ~12 for larger cations, e.g. the heavy alkaline earths and the rare-earths. In compounds with high NH_3 content, the coordination sphere is usually filled with NH_3, and the BH_4^- acts as counter ions.

4. Metal borohydrides as electrolytes

It was recently discovered that metal borohydrides could be employed as electrolytes in both the liquid and solid-state for battery applications. The reducing nature of metal borohydrides offers compatibility with metal anodes, and the low density and softness of the materials may result in high gravimetric energy-density battery cells with easy manufacturing of the electrode-electrolyte interface [24,149,150]. To be useful for solid-state electrolyte (SSE) applications, a conductivity of $\sigma > 10^{-4}$ S cm^{-1} is often mentioned as a requirement, along with a negligible electronic conductivity.

The discovery of the high-temperature polymorph of $LiBH_4$ as a super-ionic conductor initiated the research on this new class of solid-state electrolytes. At temperatures above 115 °C, $LiBH_4$ undergoes a polymorphic transition from an orthorhombic structure with a low ionic conductivity, $\sigma(Li^+) \approx 10^{-8}$ S cm^{-1} at 30 °C, to a hexagonal structure with a Li^+ conductivity of $\sigma(Li^+) \approx 10^{-3}$ S cm^{-1} at 120 °C [151]. Several approaches have been implemented to retain the high conductivity at room temperature, including the formation of dianionic compounds, e.g. $Li_4(BH_4)_3I$, $Li_2(BH_4)(NH_2)$, and $LiBH_4$:$Li_2P_2S_5$, nanoconfinement, e.g. $LiBH_4$ or $Li_4(BH_4)_3I$ in mesoporous SiO_2, and formation of dimetallic borohydrides, e.g. $LiRE(BH_4)_3Cl$ (RE^{3+} = La, Ce, Pr, Nd, Sm, Gd). These approaches have been quite successful and have increased the conductivity by several orders of magnitude as compared to $LiBH_4$, which is well described in other reviews such as ref. [46,152,153]. Recently, a new approach involves the addition of neutral ligands to improve the ionic conductivity, which will be the focus of this chapter. This research has also provided a new cation conductivity mechanism, where the ligand assists the cation migration. The ionic conductivity of this new type of ionic conductors is compared to other state-of-the-art systems based on the above-mentioned approaches in Fig. 6.

4.1. Lithium-based electrolytes

The first reported attempt to improve the ionic conductivity by adding a neutral ligand was by hydration of $LiBH_4$ to form the monohydrate $LiBH_4 \cdot H_2O$ [154]. The hydrated compound improved the RT conductivity by around two orders of magnitude compared to $LiBH_4$ and obtained a maximum value of $\sigma(Li^+) = 4.89 \cdot 10^{-4}$ S cm^{-1} at 45 °C, after which water was released from the structure, and the conductivity approached that of $LiBH_4$. ^7Li NMR was further used to verify the high Li^+ conductivity of the hydrated compound. Despite the improvement in ionic conductivity, the presence of water was reported to form an increase in resistance towards the lithium electrodes.

Later, a study on ammine lithium borohydrides showed that careful control of the ammonia content in $LiBH_4 \cdot xNH_3$ ($0 < x < 2$) could significantly change the ionic conductivity, reaching a maximum of $\sigma(Li^+) = 2.21 \cdot 10^{-3}$ S cm^{-1} at $T = 40$ °C for $LiBH_4 \cdot NH_3$ [73]. The high Li^+ conductivity was attributed to the structural changes caused by NH_3 ab/desorption, which would introduce Schottky defects and changes in the atomic environment [73]. However, a new compound with the composition $LiBH_4 \cdot \frac{1}{2}NH_3$ was later discovered, which exhibited a similar high conductivity, suggesting that the increase in
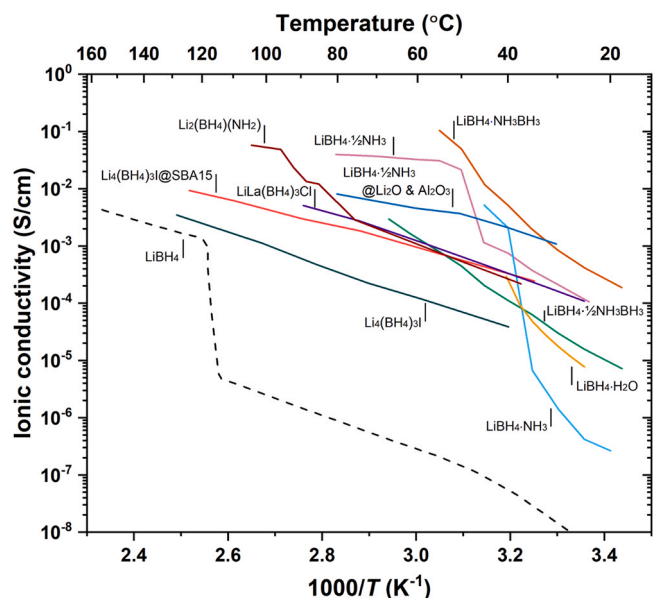
Fig. 6. Temperature-dependent Li-ion conductivity of selected complex hydrides.

conductivity may instead be due to this particular composition [50]. A migrational pathway was established based on crystal structure analysis and DFT calculations, which suggests that interstitial Li^+ can move in the interlayers in the two-dimensional structure. The high conductivity of the interstitial Li^+ is a result of a highly flexible structure owing to di-hydrogen bonds, $N-H^{\delta+}\cdots^{-\delta}H-B$, where BH_4^- groups can reorient to stabilize the coordination of both framework and interstitial Li^+, while the NH_3 can be relatively freely exchanged between the two to promote the migration of interstitial Li^+ [50].

Two different approaches have been used to produce $LiBH_4 \cdot \frac{1}{2}NH_3$, either by careful removal of ammonia from $LiBH_4 \cdot NH_3$ under vacuum, or via the mechanochemically induced reaction of $LiBH_4$, $LiNH_2$, and $LiOH$, where the latter also provided Li_2O nanoparticles, which appeared to thermally stabilize the compound [50]. The latter approach was further developed by the addition of Al_2O_3 nanoparticles, and $LiBH_4 \cdot \frac{1}{2}NH_3@Li_2O$ mixed with 60 wt% Al_2O_3 nanoparticles achieved a conductivity of $\sigma(Li^+) = 1.1 \cdot 10^{-3}$ S cm^{-1} at $T = 30$ °C [155]. The specific NH_3 content was adjusted in $LiBH_4 \cdot xNH_3@Li_2O$ ($0.67 < x < 0.8$), where a conductivity of $\sigma(Li^+) = 5.4 \cdot 10^{-4}$ S cm^{-1} was achieved at $T = 20$ °C for $x = 0.67$ with 78 wt% Li_2O [156].

The larger ligand ammonia borane (NH_3BH_3) has also resulted in a high ionic conductivity at 25 °C in $LiBH_4 \cdot xNH_3BH_3$, reaching values of $\sigma(Li^+) = 4.04 \cdot 10^{-4}$ S cm^{-1} for $x = 1$ and $\sigma(Li^+) = 1.47 \cdot 10^{-5}$ S cm^{-1} for $x = \frac{1}{2}$ [71]. The former marks the highest reported conductivity of a $LiBH_4$ based compound with $\sigma(Li^+) = 0.1$ S cm^{-1} at $T = 55$ °C.

The Li^+ transference number (t^+), i.e. the fraction of the total current arising from Li^+ migration, should ideally be unity for solid-state electrolytes to minimize or avoid polarization in the battery cell. For $LiBH_4$-based systems, the Li^+ transference number was estimated to be around $t^+ \sim 0.90$–0.96 for nanoconfined $LiBH_4$, while for $LiBH_4 \cdot NH_3BH_3$ measured at 40 °C and $LiBH_4 \cdot \frac{1}{2}NH_3BH_3$ measured at 50 °C, it was $t^+ \sim 1$ [71,157]. In other systems, e.g. $LiBH_4 \cdot 0.67NH_3@Li_2O$ [156] and $LiBH_4 \cdot \frac{1}{2}NH_3@Li_2O$-$Al_2O_3$ [155], the Li^+ transference number was not reported, instead, a five and four orders of magnitude lower electronic conductivity than the total conductivity were reported, respectively.

Although $LiBH_4$-based compounds with neutral ligands have shown promising results for their use as solid-state electrolytes, no full battery cells have yet been assembled. However, galvanostatic cycling in symmetric Li|SSE|Li cells has been demonstrated,

indicating a good compatibility with Li metal [71,155,156]. For comparison, several all-solid-state batteries have been demonstrated on other LiBH$_4$-based systems. This includes nanoconfined LiBH$_4$ with a sulfur-carbon composite cathode that had a discharge capacity of 3100 mAh g^{-1} on the 1st discharge and 1220 mAh g^{-1} after 40 cycles at 0.03 C and $T = 55\,°C$ [157]. The dianionic compounds Li$_4$(BH$_4$)$_3$I [158] and Li$_4$(BH$_4$)$_3$Cl [159] have also been used as solid-state electrolytes in full cells. Li$_4$(BH$_4$)$_3$I was assembled with lithium-titanate oxide (LTO) as the cathode and cycled at 0.2 C and $T = 150\,°C$ with 170 mAh g^{-1} and 158 mAh g^{-1} on the 1st and 2nd cycle, respectively [158]. A sulfur-carbon composite was employed as a cathode with Li$_4$(BH$_4$)$_3$Cl as the electrolyte and cycled at 0.03 C at $T = 100\,°C$ with a discharge capacity of 1377 mAh g^{-1} on the 1st discharge, which drops to 636 mAh g^{-1} on the 5th cycle [159]. Additionally, the dimetallic borohydride LiCe(BH$_4$)$_3$Cl was assembled with a sulfur-carbon composite cathode at 45 °C with an initial discharge capacity of 1196 mAh g^{-1} on the 1st discharge and 510 mAh g^{-1} on the 9th discharge with a C-rate of 0.01 [160]. More examples on borohydride based batteries are summarised in ref. [152].

4.2. Magnesium-based electrolytes

The interest in Mg(BH$_4$)$_2$ based electrolytes was initiated with the demonstration of reversible plating/stripping of Mg^{2+} in Mg(BH$_4$)$_2$ solutions in ethereal solvents, which was the first halide-free ionic Mg^{2+} electrolyte [48]. However, for solid-state electrolyte applications, Mg(BH$_4$)$_2$ has a very low ionic conductivity of $\sigma(Mg^{2+}) < 10^{-12}$ S cm^{-1} at $T = 30\,°C$ (Fig. 7). Approaches used for improvements of LiBH$_4$-based systems have also been attempted for magnesium, and the dual-anion compounds Mg(BH$_4$)(NH$_2$) and Mg$_3$(BH$_4$)$_4$(NH$_2$)$_2$ demonstrated ionic conductivities of $\sigma(Mg^{2+}) = 10^{-6}$ S cm^{-1} at $T = 150\,°C$ [161], and $\sigma(Mg^{2+}) = 4.1 \cdot 10^{-5}$ S cm^{-1} at $T = 100\,°C$ [162], respectively. A glass-ceramic phase of Mg(BH$_4$)(NH$_2$) was reported to have a conductivity of $\sigma(Mg^{2+}) = 3 \cdot 10^{-6}$ S cm^{-1} at $T = 100\,°C$ [163].

Introducing a neutral ligand has also proven efficient for magnesium systems, and a conductivity of $\sigma(Mg^{2+}) = 6 \cdot 10^{-5}$ S cm^{-1} was reported at $T = 70\,°C$ in the ethylediamine (en) derivative, Mg(BH$_4$)$_2$·NH$_2$(CH$_2$)$_2$NH$_2$ [72]. To better understand the role of the ligand, the related halide complexes, Mg(en)$_{1X2}$ (X = Cl, I), were also investigated, showing a much lower ionic conductivity. This suggests that the BH$_4^-$ anion also plays a crucial role in the conductivity

mechanism, but a more detailed analysis will require structural solution of the compound [72].

Diglyme (dg) has also been investigated as a neutral ligand. Mg(BH$_4$)$_2$·½dg demonstrated an ionic conductivity of $\sigma(Mg^{2+}) = 2 \cdot 10^{-5}$ S cm^{-1} at $T \sim 80\,°C$, while Mg(BH$_4$)$_2$·dg displayed a lower maximum conductivity, and a significantly lower activation energy, but was found to release diglyme over time [164]. While the authors ascribe the high Mg^{2+} conductivity to the chelating ability of the flexible diglyme ligand, they discover the need for a Mg(BH$_4$)$_2$ unit, which is not solvated by the organic ligand, to enhance the thermal stability of the compound [164].

Magnesium borohydride ammonia borane, Mg(BH$_4$)$_2$·2NH$_3$BH$_3$, was later investigated, which revealed a significantly higher conductivity of $\sigma(Mg^{2+}) = 5.0 \cdot 10^{-6}$ S cm^{-1} at $T = 25\,°C$, but with a low melting point of $T \sim 47\,°C$ [70,132]. The enhanced Mg-ion conductivity was ascribed to a larger volume and distortion of the tetrahedral coordination of Mg^{2+}, which leads to an increased number of Mg^{2+} conduction pathways and interstitial positions. While the role of NH$_3$BH$_3$ is not clear, it is suggested that it can be flexibly displaced or rotated to promote Mg^{2+} migration [70].

The ammine magnesium borohydrides, Mg(BH$_4$)$_2$·xNH$_3$, resulted in one of the most promising solid inorganic Mg^{2+} electrolyte systems reported so far. Initially, the compounds with integer-values of x = 1, 2, 3, and 6 were investigated, and an increase in the Mg^{2+} conductivity by several orders of magnitude was achieved [49]. Mg(BH$_4$)$_2$·NH$_3$ exhibited the highest ionic conductivity of the series, $\sigma(Mg^{2+}) \sim 3.3 \cdot 10^{-4}$ S cm^{-1} at $T = 80\,°C$. The cationic conductivity mechanism was established based on the crystal structure and DFT calculations, which showed similarities to that of LiBH$_4$·½NH$_3$ [49,50]. The interstitial Mg^{2+} migrates along the one-dimensional Mg-BH$_4$-Mg zig-zag chains in the crystal structure, where the BH$_4^-$ complexes can reorientate and be temporarily displaced from their atomic positions. The structure is flexible partly due to a network of di-hydrogen bonds, N − H$^{\delta+}$···$^{-\delta}$H−B, which facilitates the exchange of NH$_3$ between framework and interstitial magnesium, and allows for fast Mg^{2+} migration. The weak dihydrogen interactions between the chains result in a highly flexible structure, which allows for displacement of the framework magnesium atom during migration of the interstitial Mg^{2+} ion, and this mechanism is denoted *pas-de-deux* [49]. A similar flexible structure arising from a dense dihydrogen bond network is also observed for Mg(BH$_4$)$_2$·2NH$_3$BH$_3$, Mg(BH$_4$)$_2$·$x$dg and Mg(BH$_4$)$_2$·en [70,72,164].

A following investigation of composites formed by physical mixtures of two Mg(BH$_4$)$_2$·xNH$_3$ compounds with different x-values surprisingly resulted in an additional increase in the Mg-ion conductivity by about three orders of magnitude [51]. The exact reason for this increase in Mg^{2+} conductivity remains unknown. Furthermore, an eutectic molten composition x = 1.5, at $T = 55\,°C$, was also discovered, and the highest conductivity was observed for Mg(BH$_4$)$_2$·1.6NH$_3$, $\sigma(Mg^{2+}) = 2.2 \cdot 10^{-3}$ S cm^{-1} at $T = 55\,°C$, which is the highest reported value for an inorganic solid-state Mg^{2+} conductor. However, the Mg-ion conductivity rapidly decreased to $\sigma(Mg^{2+}) = 2.0 \cdot 10^{-7}$ S cm^{-1} at 25 °C, but the eutectic molten state could be stabilized by confinement with MgO nanoparticles, which resulted in $\sigma(Mg^{2+}) = 1.2 \cdot 10^{-5}$ S cm^{-1} at 25 °C. In addition to the higher conductivity at room temperature, the nanoparticles prevented recrystallization of the highly dynamical amorphous state, which is stabilized over a long period of time, i.e. several months. In contrast, the eutectic melt without nanoparticles slowly recrystallizes at room temperature, resulting in a lower conductivity [51].

The Mg(BH$_4$)$_2$ based electrolytes display an oxidative stability of around 1.2 V as determined by cyclic voltammetry in a two-electrode setup with Mg as the counter/reference electrode and Pt, Mo and Au as working electrodes for Mg(BH$_4$)$_2$·NH$_2$(CH$_2$)$_2$NH$_2$ [72], Mg(BH$_4$)$_2$·2NH$_3$BH$_3$ [70], and Mg(BH$_4$)$_2$·1.6NH$_3$@MgO [51], respectively. Upon cycling, Mg(BH$_4$)$_2$·1.6NH$_3$ was reported to form a stable
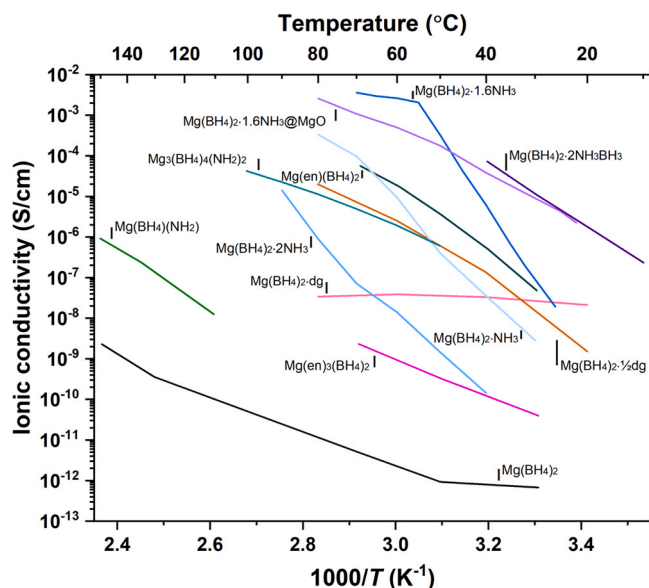

Fig. 7. Temperature-dependent Mg-ion conductivity of selected complex hydrides.

interface, which increased the stability up to 2.5 V, while facilitating Mg plating and stripping [51]. Only one $Mg(BH_4)_2$-based battery cell with a neutral ligand has been published, using Mg $(BH_4)_2 \cdot NH_2(CH_2)_2NH_2$ as the electrolyte and LTO as the cathode, where one discharge was achieved [72]. Thus, a rechargeable full battery cell based on these systems still remains to be demonstrated.

4.3. Calcium-based electrolytes

There are only a few examples of calcium-based electrolytes, and reversible Ca electrodeposition has proven challenging, e.g. passivating layers are easily formed from common Ca-salts such as Ca $(ClO_4)_2$ and $Ca(BF_4)_2$ [165]. The first report of reversible Ca plating/stripping was measured at 100 °C using $Ca(BF_4)_2$ in ethylene/propylene carbonate as a liquid electrolyte, and the temperature was sufficient to overcome the poor Ca^{2+} diffusion in the formed CaF_2 interface layer on the Ca-anode [166]. Later, it was reported that Ca $(BH_4)_2$ in THF demonstrated reversible Ca plating/stripping even at RT, with a relatively high coulombic efficiency of 94.8%, where a CaH_2 interface was formed [167]. The reversible Ca-electrodeposition was later reconfirmed, and an electrochemical deposition mechanism was proposed [168]. Addition of $LiBH_4$ can improve the desolvation of $Ca(BH_4)_2$ in THF, resulting in an improved plating/stripping cyclability and an increased coulombic efficiency of 99.1% [169]. The $Ca(BH_4)_2$-$LiBH_4$-THF mixture was further used as an electrolyte in a full battery cell using LTO as the cathode material [169].

Although promising results have been demonstrated for borohydride-based Ca-electrolytes in the liquid state, there are no reports of solid-state Ca^{2+} conductivity in $Ca(BH_4)_2$-based materials. Possibly the Ca^{2+} ion is too large for migration in these materials, while the +2 charge also results in a relatively strong electrostatic interaction with the anion lattice. Moreover, Ca^{2+} is often coordinated by six ligands in an octahedral geometry in the metal borohydride derivatives, in contrast to Mg^{2+} which can coordinate to 4, 5 and 6 ligands [24]. Thus, more interstitial positions are available in Mg-systems. However, a recent report suggests that weaker coordinating anions may facilitate Ca^{2+} mobility in the solid state, e.g. $CaB_{12}H_{12}$ and $Ca(CB_{11}H_{12})_2$ [170].

5. Dynamical investigations of metal borohydrides

Dynamical investigations on metal borohydrides are used to analyze rotational dynamics, diffusion constants or jump processes of the hydrogen species, typically by NMR or neutron techniques, e.g. quasielastic neutron scattering (QENS). For neutron investigations, hydrogen (^1H) has such a large incoherent scattering cross section that it overshadows all other probes and is usually substituted by deuterium (^2H = D) if other species are part of the investigation. While many of the derivatives of the metal borohydrides exhibit enhanced ionic conductivities, structural differences between the pure metal borohydrides also influence the conductivity. This is evident from the dynamical investigation of the amorphous phase of $Mg(BH_4)_2$, which shows a slightly higher Mg^{2+} conductivity compared to γ-$Mg(BH_4)_2$ [131]. The pattern of the scattering function S $(Q, \Delta E)$ showed that the inelastic and quasielastic contributions are dependent on the local structure of the two phases probed, γ-Mg $(BH_4)_2$ and amorphous $Mg(BH_4)_2$. The former shows almost no stochastic motions and no broadening around the elastic line, while the latter shows a significant broadening, which was explained with a higher rotational movement of the BH_4 tetrahedra [131]. Thus, with a higher number of rotating BH_4 tetrahedra, it seems likely that this motion, known as the paddlewheel effect [66], is responsible for the higher conductivity. The dynamically active BH_4 groups result in around two orders of magnitude higher conductivity at 80 °C, while a recrystallization from amorphous to γ-$Mg(BH_4)_2$ at 100 °C results

in the BH_4 tetrahedra becoming inactive, and the conductivity decreases to the same level as γ-$Mg(BH_4)_2$ [131]. Although the dynamics of $Mg(BH_4)_2$ has been investigated previously, the focus here was to define the similarities of linear $H_2BH_2 - Mg - H_2BH_2$ chains in amorphous and γ-$Mg(BH_4)_2$ [171,172]. All polymorphs of $Mg(BH_4)_2$ have also been investigated by inelastic neutron scattering (INS), revealing distinct vibrational spectra [173]. A summary of structures and dynamics can be found in ref [174].

Adding an insulating nanosized or nanoporous material to a metal borohydride can also improve the dynamical properties. An example is the composite 30/70 wt% $LiBH_4$/SiO_2 aerogel. QENS and NMR reveal two fractions of $LiBH_4$ with different mobilities of both Li and H [175]. One of the fractions accounts for the high ionic conductivity of 0.1 mS cm^{-1} at room temperature in the composite, due to increased mobility compared to the second fraction (o-$LiBH_4$). The increased mobility is caused by the interaction between $LiBH_4$ and the SiO_2 surface. Optimizing the surface contact without compromising the bulk percolation may improve the ionic conductivity further, e.g. for the 30/70 wt% composite where the fraction of ions with high mobility is only ~10% [175]. Other noteworthy composites that exhibit similar properties are nanoconfined $LiBH_4$-LiI/Al$_2O_3$, $LiBH_4$-C_{60} and $NaBH_4$-C_{60} nanocomposites, and $LiBH_4$ with nanosized oxides [176–178].

A series of dimetallic borohydride-halides $LiLa(BH_4)_3X$ (X = Cl, Br, I) also show interesting dynamic properties. Fast Li$^+$ ionic conductivity was initially assigned to the fact that only 2/3 of the available lithium positions are occupied [45]. Later, static solid-state ^7Li and ^{11}B NMR measured on $LiLa(BH_4)_3Cl$ revealed that the dynamics of BH_4^- and the migrating Li$^+$ is on the same frequency scale, suggesting that the high mobility is due to the 'paddle wheel' cationic conductivity mechanism [67]. The dimetallic borohydride-halides $LiLa(BH_4)_3X$ (X = Cl, Br, I) all exhibit very fast BH_4^- reorientation [67–70]. Increasing the radius of the halide ion results in faster reorientations of the BH_4^- anion as observed by NMR. Additionally, the activation energies for Li$^+$ diffusion derived from spin-lattice relaxation data are in good agreement with the activation energies obtained from the ionic conductivity measurements [69,103]. However, while the reorientations of the BH_4^- anions become faster with increasing halide ionic radius, the Br-based compound has the highest ionic conductivity due to a more uniform cation diffusion path [67,69].

As discussed in Chapter 4, the addition of neutral ligands can significantly enhance the ionic conductivity, which may also correlate with the observed dynamics. QENS and solid-state NMR based investigations of $Mg(BH_4)_2 \cdot \frac{1}{2}dg$ revealed the presence of two dynamically distinct BH_4^- groups. One of the BH_4^- complexes rotates relatively slowly, while the other undergoes fast isotropic jump reorientations around the C_2 and C_3 symmetry axes of BH_4^-, see Fig. 8 [164]. The slowly rotating BH_4^- group may be the reason for the greater thermal stability of $Mg(BH_4)_2 \cdot \frac{1}{2}dg$ compared to $Mg(BH_4)_2 \cdot dg$, as the inhibited dynamics of one of the BH_4^- groups is beneficial for balancing the magnesium-diglyme complexes [164,179]. The
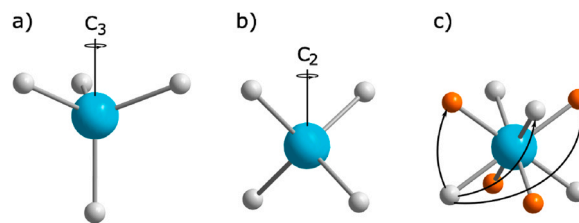

Fig. 8. Dynamics of the BH_4^- ion. a) Rotation around the C_3 symmetry axis, b) rotation around the C_2 symmetry axis, c) cubic tumbling. Color scheme: H (gray and orange), B (cyan). (For interpretation of the references to colour in this figure, the reader is referred to the web version of this article.)

compound undergoes a phase transition at 330 K, resulting in faster dynamics of the slowly rotating BH_4^- group and an increase in the flexibility of diglyme [164]. Recent investigations on $Y(BH_4)_3 \cdot xNH_3$ also reveal that the ammonia content significantly affects the dynamics of the BH_4^- group. INS spectra of the three compounds α-Y ($^{11}BH_4$)$_3$, α-Y($^{11}BH_4$)$_3 \cdot 3NH_3$, and Y($^{11}BH_4$)$_3 \cdot 7NH_3$ show that varying ammonia content only has a minor effect on the vibrational modes of ammonia. However, the vibrational modes of BH_4^- are shifted towards lower energies with increasing ammonia content due to significant changes in the local coordination of the BH_4^- group, reflecting a decreasing interaction between BH_4^- and its surroundings [146]. The librational energy decreases as BH_4^- goes from acting as a bridging bidentate ligand in α-Y(BH_4)$_3$, to coordinating to one Y^{3+} ion in α-Y(BH_4)$_3 \cdot 3NH_3$, to being only surrounded by ammonia in Y (BH_4)$_3 \cdot 7NH_3$ [146]. By partial deuteration, i.e. Y(BH_4)$_3 \cdot xND_3$ (x = 3, 7), the librational motions of BH_4^- and NH_3 could be roughly divided into three energy regions; (*i*) $^{11}BH_4^-$ librations below 55 meV, (*ii*) NH_3 librations between 55 and 130 meV, and (*iii*) ^{11}B-H and N-H bending and stretching motions above 130 meV. Both $Mg(BH_4)_2 \cdot \frac{1}{2}dg$ and Y(BH_4)$_3 \cdot xNH_3$ show that introducing neutral ligands influences the dynamics of the BH_4^- groups and thus supports this strategy for rational design of metal borohydride based compounds with high dynamics [146,164].

Obtaining information on the reorientational dynamics in systems with multiple complex components can be difficult. A prime example is NH_4BH_4, which has a dynamically ordered trigonal polymorph (*P-3*) below 45 K, where the dynamics in the system are frozen [180,181]. A polymorphic transition occurs between 45 and 50 K, together with an onset of reorientational motions of NH_4^+, which can be described as preferential tetrahedral tumbling. At 125 K, the BH_4^- becomes dynamically active and the motion can be described as cubic tumbling, see Fig. 8c [181]. Above this temperature, it is challenging to unequivocally determine the NH_4^+ motions, as these can be described as either cubic tumbling or isotropic rotational diffusion motions. The NH_4^+ and the BH_4^- ions experience different reorientationl energy barriers, and they have significantly different relaxation times. This gives rise to a cubic distribution of H positions for BH_4^- and a multitude of H positions for NH_4^+ in the cubic high temperature polymorph (*Fm-3m*) [181]. Understanding the complex dynamics in these types of systems may significantly improve the rational design and development of new materials with fast dynamics, useful as e.g. superionic conductors.

6. Other physical properties

Although metal borohydrides were initially investigated due to their high hydrogen content and potential properties as hydrogen storage materials, the focus has over the past decade been extended to a wide variety of other properties, some of which will be covered in this section.

6.1. Optical properties

A few metal borohydrides have been reported as luminescent [55–57], the first one being Eu(BH_4)$_2 \cdot 2THF$, which shows bright blue luminescence and a significant quantum yield around 75% [56]. The high quantum yield is unusual as compounds with more than 10% Eu^{2+} usually experience significant concentration quenching and thus low quantum yields due to energy transfer between the luminescent centres [56,182]. However, the borohydride anion efficiently separates the Eu^{2+} in Eu(BH_4)$_2 \cdot 2THF$ and prevents this energy transfer while the ionic character of the bonding between the BH_4^- and the Eu^{2+} ensures the blue luminescence through a small Stokes shift and d→f emission in the blue spectral region [56]. The perovskite-type metal borohydrides, KYb(BH_4)$_3$, CsEu(BH_4)$_3$, Cs$_3$Gd (BH_4)$_6$, and Cs$_2$LiGd(BH_4)$_6$ were also investigated as luminescent

materials [55]. Comparison between Eu(BH_4)$_2$ and the blue-luminescent CsEu(BH_4)$_3$ reveals a red shift of 20 nm in the latter [55]. Furthermore, studies of doping in CsCa(BH_4)$_3$ with ~5% Eu^{2+} support the minimal effect of concentration quenching in metal borohydrides as the material shows similar luminescence as CsEu(BH_4)$_3$ [55]. However, the concentration of Eu^{2+} doping in CsM(BH_4)$_3$ (M = Ca, Eu) did influence the temperature dependency of the red shift.

6.2. Magnetic properties

Magnetism requires elements with unpaired electrons in open-shell configuration to enable interactions between magnetic centers. Whereas separation of the centers is favourable for luminescent materials, the opposite is the case for permanent magnetic materials. Thus, the separation of magnetic centers created by the BH_4^- anion suggests that weak exchange interactions and thus paramagnetism is expected down to low temperatures [26]. The magnetic properties have been investigated for the entire range of the monometallic rare-earth borohydrides (except Pm) and several of the dimetallic rare-earth borohydrides [26,52,53]. However, the presence of magnetic impurities in the dimetallic compounds complicated the analysis significantly [52,53]. The monometallic rare-earth borohydrides demonstrate Curie-Weiss paramagnetic behavior with weak antiferromagnetic exchange interactions down to 3 K and magnetic moments in accord with isolated 4 f ions. Interestingly, a weak antiferromagnetic ordering was observed in Gd (BH_4)$_3$ with a Néel temperature at 4.5 K, which indicates super-exchange through the borohydride group [26]. Additionally, temperature-dependent magnetic moments were discovered as a result of low-lying excited states induced by crystal field effects [26,53].

The magnetic entropy change was researched in dimetallic gadolinium-based borohydrides due to the possible application in magnetic refrigerants [52]. Interestingly, one of the greatest entropy changes among inorganic materials was observed for K$_2$Gd(BH_4)$_5$ with 52.8 J kg$^{-1} \cdot$K^{-1} at 7 T [52]. Attempts to increase the magnetic entropy change may involve substituting the K^+ ion with a lighter one, e.g. the NH_4^+ ion.

6.3. Semiconducting metal borohydrides

Members of the perovskite-type metal borohydride group have been investigated by band gap calculations, which reveal that they are predominantly wide-gap insulators (> 5 eV) [55]. However, modifying the occupation of edge states is possible through the introduction of elements with higher-lying occupied orbitals. CsPb (BH_4)$_3$ is at present the only reported semiconducting metal borohydride, with an experimental band gap of ~1.5 eV at room temperature [55]. Compared to the other metal borohydrides, the CsPb (BH_4)$_3$ compound contains a significant amount of s(Pb) states at the valence band-edge and p(Pb) states at the conduction band edge, which creates partial covalent interactions in the Pb(BH_4)$_3$ framework through hybridization with the ligand orbitals [55]. This suggests that metal borohydride-based materials may be tuned for application in e.g. photovoltaics.

6.4. Superconductivity – theoretical predictions for LaBH$_8$

Superconductivity has been found in a range of metal hydrides exhibiting high critical temperatures (T_c) below which the compound shows superconductivity, although only at very high pressures (> 100 GPa) [183–186]. The research has culminated in the finding of superconductivity in carbonaceous sulfur hydride near room temperature (~15 °C) but at p ~ 267 GPa [183], which has triggered the hope to find a room temperature superconducting compound stable at much lower pressure. This has led attention towards the Lanthanum-Boron-Hydrogen compound, LaBH$_8$, which

is predicted by computational studies to be stable down to 40 GPa, which is considered low compared to the established compounds showing superconductivity [187]. However, the compound is yet to be proven experimentally.

6.5. Carbon capture properties

Metal borohydrides have been observed to react with gaseous CO_2, allowing the materials to be used for CO_2 sequestration or to produce valuable chemical compounds, e.g. formic acid [188,189]. The reactivity of lithium and sodium borohydride towards CO_2 was reported already in the 1950's [190–192], with the formation of formatoborohydrides, e.g.:

$$NaBH_{4\ (s)} + 2CO_{2\ (g)} \rightarrow NaBO(O_2CH)(OCH_3)_{(s)}\ T = 125\ °C \qquad (9)$$

$$NaBH_{4\ (DME)} + 3CO_{2\ (g)} \rightarrow NaBH(O_2CH)_{3\ (DME)}\ T = \text{room temperature} \qquad (10)$$
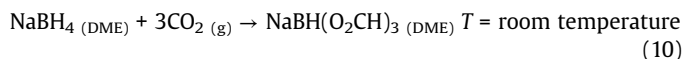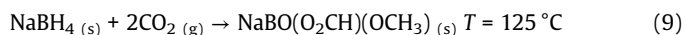
Thus highlighting that the uptake of CO_2 is dependent on the reaction conditions, which recently have received new attention [193–196].

Potassium borohydride, KBH_4, may react with CO_2 through a hydrolysis-promoted reaction, which releases H_2 and produces a carbonate containing intermediate, $K_9[B_4O_5(OH)_4]_3(CO_3)(BH_4)\cdot 7\,H_2O$ [188]. The products obtained upon complete CO_2-promoted hydrolysis are unidentified. However, the hydrolysis reaction was suggested to be utilized for CO_2 sequestration and subsequent hydrogen production [188]. Another study of KBH_4 in aqueous solution suggests the formation of primarily formic acid and a minor amount of methanol [197]. Performing the reaction during non-catalysed reactive ball-milling of KBH_4 and solid CO_2 or at elevated temperature ($< 90\ °C$) and $p(CO_2) \sim 25 - 30$ bar is also reported to form $K[H_xB(OCHO)_{4-x}]$ ($x = 1-3$) [198]. The mechanochemical treatment was followed up by a study on $LiBH_4$ and $NaBH_4$ under $p(CO_2) = 2.5$ bar, which revealed the formation of a mixture of borate, formate, and methoxy species [199].

A recent study suggests the reaction of tetraalkylammonium borohydrides with CO_2 at room temperature and low CO_2 pressure (1–3 bar) to produce liquid formatoborohydrides, i.e. tetraalkyl tri-formatoborohydride $TA[HB(OCHO)_3]^-$ [189]. Tetraethylammonium and tetrabutylammonium borohydride displayed the fastest reaction kinetics reaching 95% conversion within 20 h. The produced tetraalkyl formatoborohydrides are suggested to be used in the formation of formic acid or in solvent-free N-formylation reactions to produce ammines owing to its liquid nature [189].

Finally, the porous γ-$Mg(BH_4)_2$ proved very efficient at sorping CO_2 at mild conditions, e.g. $T = 30\ °C$ and $p(CO_2) = 1$ bar and subsequently reacts with CO_2 to form formate and methoxy species [200].

7. Outlook

Complex metal hydrides are a fascinating and continuously expanding class of materials, and an extensive amount of new materials has been reported in the past decade, mainly in the pursuit for high hydrogen density materials. Despite the discovery of many new hydrogen-rich boron- and nitrogen-based complex metal hydrides, reversible hydrogen release and uptake remain a major obstacle towards practical use of these compounds for solid-state hydrogen storage. However, a large number of other interesting properties have been discovered in the process, which is the focus of this review, including high ionic conductivity, luminescence, magnetism, semi- and superconductivity, gas-sorption and their use as reducing agents for CO_2 reduction, see Fig. 9.

Metal borohydrides, and derivatives thereof, have extremely rich chemistry, including a wide range of compositions and structural flexibility. Here we have discussed recent trends in synthesis of novel metal borohydrides, where e.g. solvent-mediated synthesis may allow for more pure products, valuable for further synthesis and characterization of the chemical and physical properties. The crystal structures of metal borohydrides are extremely diverse due to the complex nature of the BH_4^- anion, and polymorphism is often observed, e.g. as in $Mg(BH_4)_2$. New compositions and crystal structures are continuously discovered, and recent focus has been on metal borohydrides with neutral ligands, which further increases the range of possible combinations and new structural prototypes.

Hydrogen release by thermolysis from hydrogen-rich compounds and composites usually occurs readily, but hydrogen uptake is hampered by the formation of a rather thermodynamically stable dehydrogenated state. However, many different reactive hydride composite (RHC) systems have been investigated in the past, and others may be discovered in the future. They usually have high hydrogen content and low hydrogen release temperature, e.g. ~300 °C for $2NaBH_4$–MgH_2 (9.9 wt% H) [202], $Ca(BH_4)_2$–MgH_2 (10.5 wt% H) [203,204], $4LiBH_4$–MgH_2–Al (12.9 wt% H) [205], or ~340 °C for $2LiBH_4$–Al (11.4 wt% H) [206,207]. These composites store hydrogen reversibly, but only exhibit moderate kinetics and stability over several cycles of release and uptake of hydrogen. Hydrogen may also be released by a hydrolysis reaction, and $NaBH_4$ kept as a slurry in basic solution still attracts significant interest for hydrogen storage, but it appears that a catalyst is needed to accelerate and control the hydrolysis reaction [208]. The challenge for hydrogen storage in these materials is that the 'spent fuel' is another composite material, 'boron-oxide-hydroxide-hydrate', which is challenging to regenerate. This reaction product is similar to that obtained when metal borohydrides are used for CO_2 conversion and they may be converted back to a metal borohydride using hydrogen and molten magnesium.

The many newly discovered compounds are extensively studied for new interesting properties, where in particular, the fast ionic conductivity has received much focus lately. In the past decade, $LiBH_4$ and derivatives thereof, have received significant attention, and the potential use in all-solid-state batteries has been demonstrated by several examples. Importantly, the metal borohydrides appear to be stable towards metallic anodes, which is important for the realization of highly energy-dense batteries. Recently, some lithium and magnesium borohydride complexes with neutral ligands have shown to be fast ionic conductors. While many compounds have demonstrated high Li^+ conductivity, also in the solid state, there are only few reports of fast solid-state Mg^{2+} conductors, due to the stronger interactions of divalent cations with the anion lattice. Indeed, magnesium borohydride derivatives is the only class of materials that has demonstrated a sufficiently high solid-state Mg^{2+} conductivity at ambient conditions. The reported number of magnesium borohydride derivatives with high ionic conductivity is still scarce, but significant research efforts are expected within this class of materials in the coming years, which is expected to result in breakthroughs for multivalent solid-state ionic conductors.

Classical cationic conduction mechanisms relate to more rigid anion lattices, e.g. oxides and halides, and typically thermally induced defect formation. The conductivity mechanism for the metal borohydrides with neutral ligands appears to deviate significantly. Two different conductivity mechanism have been proposed, where one explains the higher conductivity as a distortion of the local coordination environment of the framework cation, resulting in a lower energy for defect formation in the solid state [70]. The other mechanism explains the higher conductivity as a *ligand-assisted* migration of interstitial cations with an associated displacement of framework atoms, and rotation and displacement of BH_4^- complexes. In the case of $Mg(BH_4)_2\cdot NH_3$, the neutral ligand, NH_3, can be exchanged relatively freely between a migrating and framework cation. Moreover, when the neutral ligand is coordinated to the interstitial Mg^{2+} cation, the 'Mg-NH_3' couple moves a step forward,
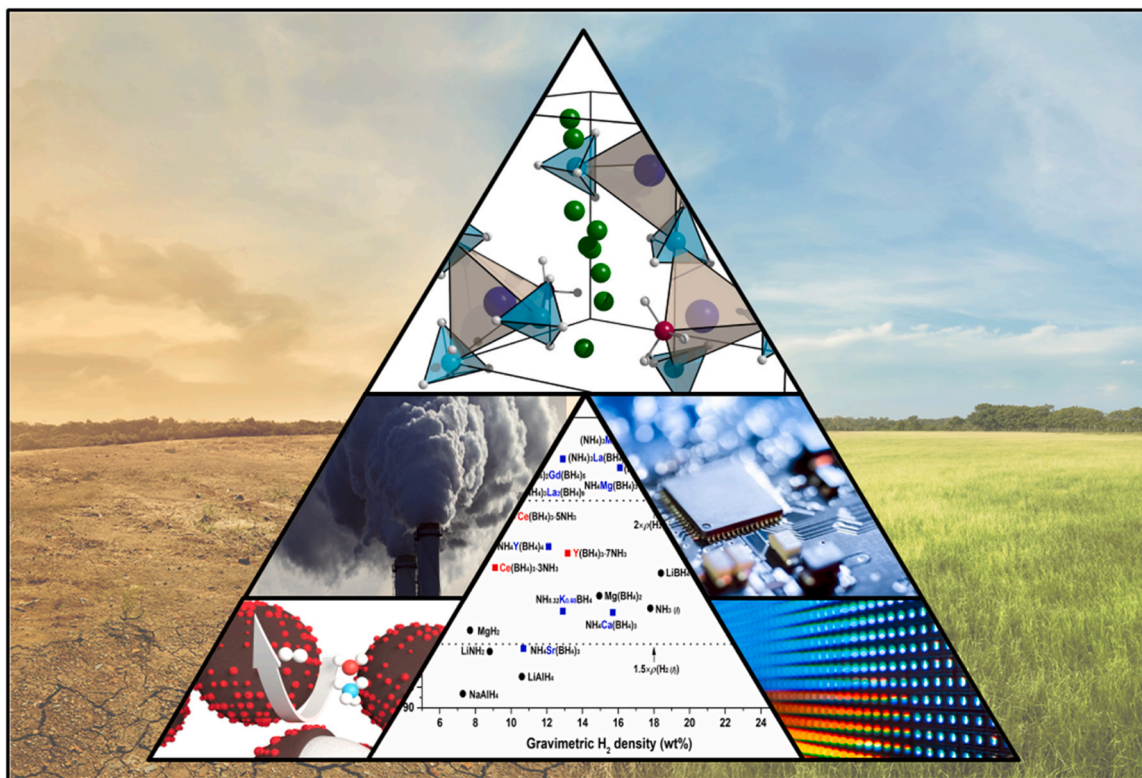
Fig. 9. Showcases of metal borohydrides: (Middle left) Carbon capture using LiBH$_4$, KBH$_4$, Mg(BH$_4$)$_2$, and tetraalkylammonium borohydride, (Bottom left) Hydrogen production using LiBH$_4$ and NaBH$_4$ [201], (Middle right) Semiconducting CsPb(BH$_4$)$_3$ with a bandgap of 1.5 eV [55], (Bottom right) Luminescent properties of Eu(BH$_4$)$_2$·2THF and perovskite-type metal borohydrides [55–57], (Bottom) Hydrogen content of various borohydrides shown as gravimetric vs. volumetric H density, (Top) Solid-state electrolytes based on LiBH$_4$ and Mg(BH$_4$)$_2$ with neutral ligands [70,155,156,163]. Ionic conduction pathway in Mg(BH$_4$)$_2$·NH$_3$ with interstitial magnesium sites marked with green. (For interpretation of the references to colour in this figure, the reader is referred to the web version of this article.)

and therefore this mechanism is denoted as *pas-de-deux* [49,50]. In this *ligand-assisted cation migration* mechanism, the framework cations are not considered as the conductivity species, but are merely temporarily displaced from their atomic positions, while an interstitial cation is migrating through the unit cell. The flexible coordination of the BH$_4^-$ complexes is crucial to stabilize both the interstitial and framework cations, and the flexible structural framework is a prerequisite for a high conductivity. An extensive network of dihydrogen bonds, e.g. N−H$^{δ+}$···$^{−δ}$H−B, is suggested to contribute to a highly flexible structure [49].

The specific effect of the neutral ligands in different structures likely depends on their chemical and physical properties, such as the geometrical shape, the interactions with its surroundings and the ability to coordinate cations, which will affect the crystal structures and the ionic conduction channels. Thus, the specific details of the cation conductivity mechanism may depend on both the crystal structure and the properties of the ligand. Structural analysis of metal borohydrides with neutral ligands reveals that the structural dimensionality of the 'M−BH$_4$' moiety is decreasing with increasing ligand content, and two-dimensional layered or one-dimensional chain-like structures are often formed by introducing a low number of ligands, which can form conduction channels in the unit cell. On the other hand, a higher number of ligands often result in even lower dimensionality and isolated molecular units or cationic complex ions, which may disrupt the conduction channels. This hypothesis appears to agree with the trend in conductivity for the Mg (BH$_4$)$_2$·xNH$_3$ (x = 1, 2, 3, 6) systems [49], but further investigations of new systems are necessary to evaluate general trends.

The addition of inert nanoparticles and mesoporous compounds has also proven to be a valuable tool to enhance the ionic conductivity of metal borohydrides. It has been widely applied for LiBH$_4$-systems, where a highly conducting state is stabilized at the interfaces [47,209–212]. Recently, it was also employed in the Mg (BH$_4$)$_2$·1.6NH$_3$ system, where it not only stabilized a highly conducting eutectic molten state to ambient conditions and prevented recrystallization, but also provided mechanical stabilization to form a solid functional electrolyte material [51].

Several borohydride-based solid-state Li batteries have been demonsted [152], but for many of the newly reported borohydride-based systems with neutral ligands, rechargeable full cells are still absent. One of the challenges for borohydride-based batteries is the limited anodic stability and initial results on the electrochemical stability of LiBH$_4$ suggested an oxidative stability of up to 5 V [46], which was much higher than the oxidative stability of 2 V obtained from DFT calculations [213, 214]. Through careful experiments with carbon additives at the working electrode, the electrochemical stability could be assessed experimentally to 2.0 V vs Li$^+$/Li [215], which stresses the importance of proper electrical contact in the assessment of new electrolyte candidates. In addition, the utilization of three-electrode cells for electrochemical testing should be employed to carefully study electrochemical processes, such as plating and stripping at the metal anode, as seen for other systems [216]. The initial high oxidative stability has been ascribed to the formation of a Li$_2$B$_{12}$H$_{12}$ interface with a higher thermal and electrochemical stability and a reasonable ionic conductivity above the LiBH$_4$ orthorhombic to hexagonal transition [217]. An electrochemically formed interface with higher electrochemical stability has similarly been observed for e.g. Mg(BH$_4$)$_2$·1.6NH$_3$ [51], which did not display any significant currents up to 2.5 V vs. Mg^{2+}/Mg after being electrochemically matured. The practical usage of borohydrides as electrolytes for solid-state batteries, especially solid-state Mg batteries, thus rely on the formation of a protective interface or the

development of compatible catholytes (i.e. electrolyte towards the cathode-side) or cathode coatings to enable a higher voltage across the cell. Similar approaches are used for the thiophosphates and argyrodites Li electrolytes, which also suffer from relatively low oxidative stabilities [218–222]. As Mg electrolytes are improving, a large array of new cathode candidates for Mg batteries are reported in the literature [223, 224]. The success of a commercial Mg battery is thus dependent on the continuous development and improvement of electrolytes, cathodes, and interfaces.

The dynamics in metal borohydrides and their relation to ionic conductivity has also been addressed in this review. The high ionic conductivity of complex metal hydrides is often related to the dynamical features within the structures, e.g. BH_4^- reorientations in $LiRE(BH_4)_3Cl$, anion rotations in metal $closo$-borates and simultaneous NH_3 and BH_4^- dynamics in $M(BH_4)_n \cdot xNH_3$ (M = Li, Mg; x = 0.5 or 1). An improved understanding of the dynamics in these materials is necessary, and dynamical studies using NMR spectroscopy and neutron scattering techniques may provide new insight into the phenomena responsible for the interesting properties. Additionally, it is of great interest to be able to model the dynamics in materials with multiple different dynamical components such as $M(CB_9H_{10})(CB_{11}H_{12})$ or metal borohydride systems with complex ligands, as this will add significantly to future rational design of solid-state fast ionic conductors.

Metal borohydrides containing unpaired electrons, e.g. the rare-earths, may also show interesting applications for solid-state luminescence and magnetic applications. A high spatial separation of the luminescent and magnetic centers (RE-ions) results in low concentration quenching and dominatingly paramagnetic exchange coupling [26,56]. However, there is a weak tendency for antiferromagnetic coupling in rare-earth metal borohydrides, and an unusual temperature dependency of the magnetic moment. Interestingly, a weak antiferromagnetic ordering has also been observed in $Gd(BH_4)_3$, being the first example of magnetic superexchange through a borohydride group [26]. The research of luminescent and magnetic properties of metal borohydrides is scarce, and further research may result in some new and interesting applications. Other niche applications that have been reported include semiconductivity in $CsPb(BH_4)_3$ [55], theoretical investigations of superconductivity, the use of metal borohydrides as reducing agents for CO_2, and gas-sorption properties in the porous γ-$Mg(BH_4)_2$.

The research presented in this review clearly demonstrates that there are still plenty of room for development of new synthesis routes and discovery of new complex hydrides, which may show unprecedented and interesting properties. Other related materials, e.g. metal hydrides and higher borates, have recently been addressed in other reviews, which also present a large variety of possible applications [225–229]. In particular, the borates show promising applications as solid-state ionic conductors, and with a higher thermal- and electrochemical stability as compared to the borohydrides. The discovery of new applications, going beyond hydrogen storage and the well-known lithium battery, breathes new life into the research on complex metal hydrides, in particular for all-solid-state batteries. An increased knowledge of trends in synthesis, structures and properties, and an improved understanding of the fundamental features responsible for a given physical property, is crucial for rational design of new materials with specific properties.

CRediT authorship contribution statement

Jakob B. Grinderslev: Writing – original draft. **Mads B. Amdisen:** Writing – original draft. **Lasse N. Skov:** Writing – original draft. **Kasper T. Møller:** Writing – original draft. **Lasse G. Kristensen:** Writing – original draft. **Marek Polanski:** Writing – original draft. **Michael Heere:** Writing - original draft. **Torben R. Jensen:** Writing - original draft, Supervision.

Declaration of Competing Interest

The authors declare that they have no known competing financial interests or personal relationships that could have appeared to influence the work reported in this paper.

Acknowledgements

References

[1] D. MacKay, Sustainable Energy - Without the Hot Air, UIT Cambridge, 2008, ⟨http://www.dspace.cam.ac.uk/handle/1810/217849⟩.

[2] M.B. Ley, L.H. Jepsen, Y.-S. Lee, Y.W. Cho, J.M. Bellosta von Colbe, M. Dornheim, M. Rokni, J.O. Jensen, M. Sloth, Y. Filinchuk, J.E. Jørgensen, F. Besenbacher, T.R. Jensen, Complex hydrides for hydrogen storage – new perspectives, Mater. Today 17 (3) (2014) 122–128, https://doi.org/10.1016/j.mattod.2014.02.013

[3] J. Bellosta von Colbe, J.-R. Ares, J. Barale, M. Baricco, C. Buckley, G. Capurso, N. Gallandat, D.M. Grant, M.N. Guzik, I. Jacob, E.H. Jensen, T. Jensen, J. Jepsen, T. Klassen, M.V. Lototskyy, K. Manickam, A. Montone, J. Puszkiel, S. Sartori, D.A. Sheppard, A. Stuart, G. Walker, C.J. Webb, H. Yang, V. Yartys, A. Züttel, M. Dornheim, Application of hydrides in hydrogen storage and compression: achievements, outlook and perspectives, Int. J. Hydrog. Energy 44 (15) (2019) 7780–7808, https://doi.org/10.1016/j.ijhydene.2019.01.104

[4] E. Hadjixenophontos, E.M. Dematteis, N. Berti, A.R. Wołczyk, P. Huen, M. Brighi, T.T. Le, A. Santoru, S. Payandeh, F. Peru, A.H. Dao, Y. Liu, M. Heere, A Review of the MSCA ITN ECOSTORE-novel complex metal hydrides for efficient and compact storage of renewable energy as hydrogen and electricity, Inorganics 8 (3) (2020) 17, https://doi.org/10.3390/inorganics8030017

[5] J.F. Stampfer, C.E. Holley, J.F. Suttle, The magnesium–hydrogen system$^{1-3}$, J. Am. Chem. Soc. 82 (14) (1960) 3504–3508, https://doi.org/10.1021/ja01499a006

[6] M. Polanski, T.K. Nielsen, Y. Cerenius, J. Bystrzycki, T.R. Jensen, Synthesis and decomposition mechanisms of Mg_2FeH_6 studied by in-situ synchrotron x-ray diffraction and high-pressure DSC, Int. J. Hydrog. Energy 8 (35) (2010) 3578–3582, https://doi.org/10.1016/j.ijhydene.2010.01.144

[7] B. Bogdanović, A. Reiser, K. Schlichte, B. Spliethoff, B. Tesche, Thermodynamics and dynamics of the Mg–Fe–H system and its potential for thermochemical thermal energy storage, J. Alloy. Compd. 1–2 (345) (2002) 77–89, https://doi.org/10.1016/S0925-8388(02)00308-0

[8] J.A. Puszkiel, P.A. Larochette, F.C. Gennari, Thermodynamic and Kinetic Studies of Mg–Fe–H after mechanical milling followed by sintering, J. Alloy. Compd. 1–2 (463) (2008) 134–142, https://doi.org/10.1016/j.jallcom.2007.08.085

[9] J.A. Puszkiel, P. Arneodo Larochette, F.C. Gennari, Hydrogen storage properties of Mg_xFe (x: 2, 3 and 15) compounds produced by reactive ball milling, J. Power Sources 186 (1) (2009) 185–193, https://doi.org/10.1016/j.jpowsour.2008.09.101

[10] J. Puszkiel, F. Gennari, P.A. Larochette, C. Pistidda, R. Gosalawit-Utke, J. Jepsen, T.R. Jensen, C. Gundlach, J.B. von Colbe, T. Klassen, M. Dornheim, Sorption behavior of the MgH_2–Mg_2FeH_6 hydride storage system synthesized by mechanical milling followed by sintering, Int. J. Hydrog. Energy 38 (34) (2013) 14618–14630, https://doi.org/10.1016/j.ijhydene.2013.08.068

[11] I.G. Fernández, G.O. Meyer, F.C. Gennari, Hydriding/dehydriding behavior of Mg_2CoH_5 produced by reactive mechanical milling, J. Alloy. Compd. 464 (1) (2008) 111–117, https://doi.org/10.1016/j.jallcom.2007.09.102

[12] M. Norek, T.K. Nielsen, M. Polanski, I. Kunce, T. Płociński, L.R. Jaroszewicz, Y. Cerenius, T.R. Jensen, J. Bystrzycki, Synthesis and decomposition mechanisms of ternary Mg_2CoH_5 studied using in situ synchrotron x-ray diffraction, Int. J. Hydrog. Energy 36 (17) (2011) 10760–10770, https://doi.org/10.1016/j.ijhydene.2011.05.126

[13] M.G. Verón, F.C. Gennari, Thermodynamic behavior of the Mg–Co–H system: the effect of hydrogen cycling, J. Alloy. Compd. 614 (2014) 317–322, https://doi.org/10.1016/j.jallcom.2014.06.092

[14] C. Zlotea, Y. Oumellal, J.J.S. Berrú, K.-F. Aguey-Zinsou, On the feasibility of the bottom-up synthesis of Mg2CoH5 nanoparticles supported on a porous carbon and their hydrogen desorption behaviour, Nano Struct. Nano Objects 16 (2018) 144–150, https://doi.org/10.1016/j.nanoso.2018.05.010

[15] J. Barale, S. Deledda, E.M. Dematteis, M.H. Sørby, M. Baricco, B.C. Hauback, Synthesis and characterization of magnesium-iron-cobalt complex hydrides, Sci. Rep. 10 (1) (2020) 9000, https://doi.org/10.1038/s41598-020-65774-8

[16] M. Polanski, T.K. Nielsen, I. Kunce, M. Norek, T. Płociński, L.R. Jaroszewicz, C. Gundlach, T.R. Jensen, J. Bystrzycki, Mg_2NiH_4 synthesis and decomposition

reactions, Int. J. Hydrog. Energy 38 (10) (2013) 4003–4010, https://doi.org/10.1016/j.ijhydene.2013.01.119

[17] J.J. Vajo, S.L. Skeith, F. Mertens, Reversible storage of hydrogen in destabilized LiBH$_4$, J. Phys. Chem. B 109 (9) (2005) 3719–3722, https://doi.org/10.1021/jp040769o

[18] P. Mauron, F. Buchter, O. Friedrichs, A. Remhof, M. Bielmann, C.N. Zwicky, A. Züttel, Stability and reversibility of LiBH$_4$, J. Phys. Chem. B 112 (3) (2008) 906–910, https://doi.org/10.1021/jp077572r

[19] U. Bösenberg, S. Doppiu, L. Mosegaard, G. Barkhordarian, N. Eigen, A. Borgschulte, T.R. Jensen, Y. Cerenius, O. Gutfleisch, T. Klassen, M. Dornheim, R. Bormann, Hydrogen sorption properties of MgH$_2$–LiBH$_4$ composites, Acta Mater. 55 (11) (2007) 3951–3958, https://doi.org/10.1016/j.actamat.2007.03.010

[20] P. Martelli, R. Caputo, A. Remhof, P. Mauron, A. Borgschulte, A. Züttel, Stability and decomposition of NaBH$_4$, J. Phys. Chem. C 114 (15) (2010) 7173–7177, https://doi.org/10.1021/jp909341z

[21] A. Karkamkar, S.M. Kathmann, G.K. Schenter, D.J. Heldebrant, N. Hess, M. Gutowski, T. Autrey, Thermodynamic and structural investigations of ammonium borohydride, a solid with a highest content of thermodynamically and kinetically accessible hydrogen, Chem. Mater. 21 (19) (2009) 4356–4358, https://doi.org/10.1021/cm902385c

[22] J.B. Grinderslev, L.H. Jepsen, Y.-S. Lee, K.T. Møller, Y.W. Cho, R. Černý, T.R. Jensen, Structural diversity and trends in properties of an array of hydrogen-rich ammonium metal borohydrides, Inorg. Chem. 59 (17) (2020) 12733–12747, https://doi.org/10.1021/acs.inorgchem.0c01797

[23] G. Soloveichik, J.-H. Her, P.W. Stephens, Y. Gao, J. Rijssenbeek, M. Andrus, J.-C. Zhao, Ammine magnesium borohydride complex as a new material for hydrogen storage: structure and properties of Mg(BH$_4$)$_2$·2NH$_3$, Inorg. Chem. 47 (10) (2008) 4290–4298, https://doi.org/10.1021/ic7023633

[24] M. Paskevicius, L.H. Jepsen, P. Schouwink, R. Černý, D.B. Ravnsbæk, Y. Filinchuk, M. Dornheim, F. Besenbacher, T.R. Jensen, Metal borohydrides and derivatives – synthesis, structure and properties, Chem. Soc. Rev. 46 (5) (2017) 1565–1634, https://doi.org/10.1039/C6CS00705H

[25] R. Černý, P. Schouwink, The crystal chemistry of inorganic metal borohydrides and their relation to metal oxides, Acta Crystallogr. Sect. B B71 (6) (2015) 619–640, https://doi.org/10.1107/S2052520615018508

[26] J.B. Grinderslev, K.T. Møller, M. Bremholm, T.R. Jensen, Trends in synthesis, crystal structure, and thermal and magnetic properties of rare-earth metal borohydrides, Inorg. Chem. 58 (9) (2019) 5503–5517, https://doi.org/10.1021/acs.inorgchem.8b03258

[27] K. Suárez-Alcántara, J.R. Tena García, Metal borohydrides beyond groups I and II: a review, Materials 14 (10) (2021) 2561, https://doi.org/10.3390/ma14102561

[28] H. Hagemann, Boron hydrogen compounds for hydrogen storage and as solid ionic conductors, Chim. Int. J. Chem. 73 (11) (2019) 868–873, https://doi.org/10.2533/chimia.2019.868

[29] R.W. Parry, D.R. Schultz, P.R. Girardot, The preparation and properties of hexamminecobalt(iii) borohydride, hexamminechromium(iii) borohydride and ammonium borhydride1, J. Am. Chem. Soc. 80 (1) (1958) 1–3, https://doi.org/10.1021/ja01534a001

[30] R. Flacau, C.I. Ratcliffe, S. Desgreniers, Y. Yao, D.D. Klug, P. Pallister, I.L. Moudrakovski, J.A. Ripmeester, Structure and dynamics of ammonium borohydride, Chem. Commun. 46 (48) (2010) 9164–9166, https://doi.org/10.1039/C0CC03297B

[31] T.K. Nielsen, A. Karkamkar, M. Bowden, F. Besenbacher, T.R. Jensen, T. Autrey, Methods to stabilize and destabilize ammonium borohydride, Dalton Trans. 42 (3) (2013) 680–687, https://doi.org/10.1039/C2DT31591B

[32] A. Starobrat, T. Jaroń, W. Grochala, New hydrogen-rich ammonium metal borohydrides, NH$_4$[M(BH$_4$)$_4$], M = Y, Sc, Al, as potential H$_2$ sources, Dalton Trans. 47 (13) (2018) 4442–4448, https://doi.org/10.1039/C7DT03926C

[33] I. Dovgaliuk, D.A. Safin, N.A. Tumanov, F. Morelle, A. Moulai, R. Černý, Z. Łodziana, M. Devillers, Y. Filinchuk, Solid aluminum borohydrides for prospective hydrogen storage, ChemSusChem 10 (23) (2017) 4725–4734, https://doi.org/10.1002/cssc.201701629

[34] L.H. Jepsen, M.B. Ley, Y.-S. Lee, Y.W. Cho, M. Dornheim, J.O. Jensen, Y. Filinchuk, J.-E. Jørgensen, F. Besenbacher, T.R. Jensen, Boron-nitrogen based hydrides and reactive composites for hydrogen storage, Mater. Today 17 (4) (2014) 129–135, https://doi.org/10.1016/j.mattod.2014.02.015

[35] L.H. Jepsen, Y.-S. Lee, R. Černý, R.S. Sarusie, Y.W. Cho, F. Besenbacher, T.R. Jensen, Ammine calcium and strontium borohydrides: syntheses, structures, and properties, ChemSusChem 8 (20) (2015) 3472–3482, https://doi.org/10.1002/cssc.201500713

[36] L.H. Jepsen, M.B. Ley, Y. Filinchuk, F. Besenbacher, T.R. Jensen, Tailoring the properties of ammine metal borohydrides for solid-state hydrogen storage, ChemSusChem 8 (8) (2015) 1452–1463, https://doi.org/10.1002/cssc.201500029

[37] M. Dornheim, N. Eigen, G. Barkhordarian, T. Klassen, R. Bormann, Tailoring hydrogen storage materials towards application, Adv. Eng. Mater. 8 (5) (2006) 377–385, https://doi.org/10.1002/adem.200600018

[38] M.B. Smith, G.E. Bass, Heats and free energies of formation of the alkali aluminum hydrides and of cesium hydride, J. Chem. Eng. Data 8 (3) (1963) 342–346, https://doi.org/10.1021/je60018a020

[39] M. Paskevicius, D.A. Sheppard, C.E. Buckley, Thermodynamic changes in mechanochemically synthesized magnesium hydride nanoparticles, J. Am. Chem. Soc. 132 (14) (2010) 5077–5083, https://doi.org/10.1021/ja908398u

[40] S.V. Alapati, J.K. Johnson, D.S. Sholl, Identification of destabilized metal hydrides for hydrogen storage using first principles calculations, J. Phys. Chem. B 110 (17) (2006) 8769–8776, https://doi.org/10.1021/jp060482m

[41] G.A. Olah, Beyond oil and gas: the methanol economy, Angew. Chem. Int. Ed. Engl. 44 (18) (2005) 2636–2639, https://doi.org/10.1002/anie.200462121

[42] IRENA AND METHANOL INSTITUTE (2021). Innovation Outlook: Renewable Methanol.

[43] L. Lombardo, H. Yang, K. Zhao, P.J. Dyson, A. Züttel, Solvent- and catalyst-free carbon dioxide capture and reduction to formate with borohydride ionic liquid, ChemSusChem 13 (8) (2020) 2025–2031, https://doi.org/10.1002/cssc.201903514

[44] M. Matsuo, Y. Nakamori, S. Orimo, H. Maekawa, H. Takamura, Lithium superionic conduction in lithium borohydride accompanied by structural transition, Appl. Phys. Lett. 91 (22) (2007) 224103, https://doi.org/10.1063/1.2817934

[45] M.B. Ley, D.B. Ravnsbæk, Y. Filinchuk, Y.-S. Lee, R. Janot, Y.W. Cho, J. Skibsted, T.R. Jensen, LiCe(BH$_4$)$_3$Cl, a new lithium-ion conductor and hydrogen storage material with isolated tetranuclear anionic clusters, Chem. Mater. 24 (9) (2012) 1654–1663, https://doi.org/10.1021/cm300792t

[46] M. Matsuo, S. Orimo, Lithium fast-ionic conduction in complex hydrides: review and prospects, Adv. Energy Mater. 1 (2) (2011) 161–172, https://doi.org/10.1002/aenm.201000012

[47] D. Blanchard, A. Nale, D. Sveinbjörnsson, T.M. Eggenhuisen, M.H.W. Verkuijlen, Suwarno, T. Vegge, A.P.M. Kentgens, P.E. de Jongh, Nanoconfined LiBH$_4$ as a fast lithium ion conductor, Adv. Funct. Mater. 25 (2) (2015) 184–192, https://doi.org/10.1002/adfm.201402538

[48] R. Mohtadi, M. Matsui, T.S. Arthur, S.-J. Hwang, Magnesium borohydride: from hydrogen storage to magnesium battery, Angew. Chem. Int. Ed. Engl. 51 (39) (2012) 9780–9783, https://doi.org/10.1002/anie.201204913

[49] Y. Yan, W. Dononelli, M. Jørgensen, J.B. Grinderslev, Y.-S. Lee, Y.W. Cho, R. Černý, B. Hammer, T.R. Jensen, The mechanism of Mg^{2+} conduction in ammine magnesium borohydride promoted by a neutral molecule, Phys. Chem. Chem. Phys. 22 (17) (2020) 9204–9209, https://doi.org/10.1039/d0cp00158a

[50] Y. Yan, J.B. Grinderslev, Y.-S. Lee, M. Lee, Y.W. Cho, R. Černý, T.R. Jensen, Ammonia-assisted fast Li-Ion conductivity in a new hemiammine lithium borohydride, LiBH$_4$·1/2NH$_3$, Chem. Commun. 56 (28) (2020) 3971–3974, https://doi.org/10.1039/C9CC09990E

[51] Y. Yan, J.B. Grinderslev, M. Jørgensen, L.N. Skov, J. Skibsted, T.R. Jensen, Ammine magnesium borohydride nanocomposites for all-solid-state magnesium batteries, ACS Appl. Energy Mater. 3 (9) (2020) 9264–9270, https://doi.org/10.1021/acsaem.0c01599

[52] P. Schouwink, E. Didelot, Y.-S. Lee, T. Mazet, R. Černý, Structural and magnetocaloric properties of novel gadolinium borohydrides, J. Alloy. Compd. 664 (Suppl. C) (2016) 378–384, https://doi.org/10.1016/j.jallcom.2015.12.182

[53] W. Wegner, J. van Leusen, J. Majewski, W. Grochala, P. Kögerler, Borohydride as magnetic superexchange pathway in late lanthanide borohydrides, Eur. J. Inorg. Chem. 13 (2019) 1776–1783, https://doi.org/10.1002/ejic.201801488

[54] W. Wegner, J.J. Zakrzewski, M. Zychowicz, S. Chorazy, Incorporation of expanded organic cations in dysprosium(iii) borohydrides for achieving luminescent molecular nanomagnets, Sci. Rep. 11 (1) (2021) 11354, https://doi.org/10.1038/s41598-021-88446-7

[55] P. Schouwink, M.B. Ley, A. Tissot, H. Hagemann, T.R. Jensen, Ł. Smrčok, R. Černý, Structure and properties of complex hydride perovskite materials, Nat. Commun. 5 (2014) 5706, https://doi.org/10.1038/ncomms6706

[56] S. Marks, J.G. Heck, M.H. Habicht, P. Oña-Burgos, C. Feldmann, P.W. Roesky, [Ln(BH$_4$)$_2$(THF)$_2$] (Ln = Eu, Yb) - a highly luminescent material. synthesis, properties, reactivity, and nmr studies, J. Am. Chem. Soc. 134 (41) (2012) 16983–16986, https://doi.org/10.1021/ja308077t

[57] J. Christmann, A. Mansouri, J.B. Grinderslev, T.R. Jensen, H. Hagemann, Probing the local symmetry of Tb^{3+} in borohydrides using luminescence spectroscopy, J. Lumin. 221 (2020) 117065, https://doi.org/10.1016/j.jlumin.2020.117065

[58] I. Dovgaliuk, F. Nouar, C. Serre, Y. Filinchuk, D. Chernyshov, Cooperative adsorption by porous frameworks: diffraction experiment and phenomenological theory, Chem. Eur. J. 23 (70) (2017) 17714–17720, https://doi.org/10.1002/chem.201702707

[59] Y. Filinchuk, B. Richter, T.R. Jensen, V. Dmitriev, D. Chernyshov, H. Hagemann, Porous and dense magnesium borohydride frameworks: synthesis, stability, and reversible absorption of guest species, Angew. Chem. Int. Ed. 50 (2011) 11162–11166, https://doi.org/10.1002/anie.201100675

[60] M. Visseaux, F. Bonnet, Borohydride complexes of rare earths, and their applications in various organic transformations, Coord. Chem. Rev. (2011) 374–420, https://doi.org/10.1016/j.ccr.2010.09.016

[61] S. Fadlallah, M. Terrier, C. Jones, P. Roussel, F. Bonnet, M. Visseaux, Mixed Allyl–borohydride lanthanide complexes: synthesis of Ln(BH$_4$)$_2$(C$_3$H$_5$)(THF)$_3$ (Ln = Nd, Sm), characterization, and reactivity toward polymerization, Organometallics 35 (4) (2016) 456–461, https://doi.org/10.1021/acs.organomet.5b00877

[62] D. Barbier-Baudry, O. Blacque, A. Hafid, A. Nyassi, H. Sitzmann, M. Visseaux, Synthesis and X-Ray crystal structures of (C$_5$HiPr$_4$)Ln(BH$_4$)$_2$(THF)(Ln = Nd and Sm), versatile precursors for polymerization catalysts. Eur. J. Inorg. Chem. 2000 (11) (2000) 2333–2336, https://doi.org/10.1002/1099-0682(200011)2000:11<2333::AID-EJIC2333>3.0.CO;2-S

[63] A. Momin, F. Bonnet, M. Visseaux, L. Maron, J. Takats, M.J. Ferguson, X.-F.L. Goff, F. Nief, Synthesis and structure of divalent thulium borohydrides, and their application in ε-caprolactone polymerization, Chem. Commun. 47 (44) (2011) 12203–12205, https://doi.org/10.1039/C1CC15294G

[64] F. Jaroschik, F. Bonnet, X.-F.L. Goff, L. Ricard, F. Nief, M. Visseaux, Synthesis of samarium(II) borohydrides and their behaviour as initiators in styrene and ε-caprolactone polymerisation, Dalton Trans. 39 (29) (2010) 6761–6766, https://doi.org/10.1039/C001795G

[65] M. Paskevicius, B. Richter, M. Polański, S.P. Thompson, T.R. Jensen, Sulfurized metal borohydrides, Dalton Trans. 45 (2) (2015) 639–645, https://doi.org/10.1039/C5DT04304B

[66] M. Jansen, Volume effect or paddle-wheel mechanism-fast alkali-metal ionic conduction in solids with rotationally disordered complex anions, Angew. Chem. Int. Ed. 30 (12) (1991) 1547–1558, https://doi.org/10.1002/anie.199115471

[67] A.V. Skripov, A.V. So_onin, M.B. Ley, T.R. Jensen, Y. Filinchuk, Nuclear magnetic resonance studies of BH4 reorientations and Li diffusion in LiLa(BH4)3Cl, J. Phys. Chem. C 117 (29) (2013) 14965–14972, https://doi.org/10.1021/jp403746m

[68] A.V. Skripov, G. Majer, O.A. Babanova, R.V. Skoryunov, A.V. Soloninin, M.B. Ley, T.R. Jensen, S. Orimo, T.J. Udovic, Lithium-ion diffusivity in complex hydrides: pulsed-field-gradient NMR studies of LiLa(BH4)3Cl, Li3(NH2)2I and Li-1-CB9H10, Solid State Ion. 362 (2021) 115585, https://doi.org/10.1016/j.ssi.2021.115585

[69] A.V. Soloninin, O.A. Babanova, R.V. Skoryunov, A.V. Skripov, J.B. Grinderslev, T.R. Jensen, NMR study of the dynamical properties of LiLa(BH4)3Br and LiLa (BH4)3I, Appl. Magn. Reson. 52 (5) (2021) 595–606, https://doi.org/10.1007/s00723-021-01319-0

[70] K. Kisu, S. Kim, M. Inukai, H. Oguchi, S. Takagi, S. Orimo, Magnesium borohydride ammonia borane as a magnesium ionic conductor, ACS Appl. Energy Mater. 3 (2020) 3174–3179, https://doi.org/10.1021/acsaem.0c00113

[71] H. Liu, Z. Ren, X. Zhang, J. Hu, M. Gao, H. Pan, Y. Liu, Incorporation of ammonia borane groups in the lithium borohydride structure enables ultrafast lithium ion conductivity at room temperature for solid-state batteries, Chem. Mater. 32 (2) (2020) 671–678, https://doi.org/10.1021/acs.chemmater.9b03188

[72] E. Roedern, R.-S. Kühnel, A. Remhof, C. Battaglia, Magnesium ethylenediamine borohydride as solid-state electrolyte for magnesium batteries, Sci. Rep. 7 (2017) 46189, https://doi.org/10.1038/srep46189

[73] T. Zhang, Y. Wang, T. Song, H. Miyaoka, K. Shinzato, H. Miyaoka, T. Ichikawa, S. Shi, X. Zhang, S. Isobe, N. Hashimoto, Y. Kojima, Ammonia, a switch for controlling high ionic conductivity in lithium borohydride ammoniates, Joule 2 (8) (2018) 1522–1533, https://doi.org/10.1016/j.joule.2018.04.015

[74] H.I. Schlesinger, R.T. Sanderson, A.B. Burg, Metallo borohydrides. i. aluminum borohydride, J. Am. Chem. Soc. 62 (12) (1940) 3421–3425, https://doi.org/10.1021/ja01869a037

[75] A.B. Burg, H.I. Schlesinger, Metallo borohydrides. ii. beryllium borohydride, J. Am. Chem. Soc. 62 (12) (1940) 3425–3429, https://doi.org/10.1021/ja01869a038

[76] H.I. Schlesinger, H.C. Brown, Metallo borohydrides. iii. lithium borohydride, J. Am. Chem. Soc. 62 (12) (1940) 3429–3435, https://doi.org/10.1021/ja01869a039

[77] E. Wiberg, R. Hartwimmer, Notizen: zur kenntnis von erdalkali-tetraalk-oxoboraten Me[B(OR)4]2. Zeitschrift Fur Naturforsch. B 10 (5) (1955) 290–291, https://doi.org/10.1515/znb-1955-0509

[78] R. Köster, Neue herstellungsmethoden für metallborhydride, Angew. Chem. 69 (3) (1957) 94, https://doi.org/10.1002/ange.19570690310

[79] H. Nöth, Anorganische reaktionen der alkaliboranate, Angew. Chem. 73 (11) (1961) 371–383, https://doi.org/10.1002/ange.19610731106

[80] S.W. Chaikin, W.G. Brown, Reduction of aldehydes, ketones and acid chlorides by sodium borohydride, J. Am. Chem. Soc. 71 (1) (1949) 122–125, https://doi.org/10.1021/ja01169a033

[81] J. Kollonitsch, O. Fuchs, V. Gábor, New and known complex borohydrides and some of their applications in organic syntheses, Nature 173 (4394) (1954) 125–126, https://doi.org/10.1038/173125a0

[82] H.I. Schlesinger, H.C. Brown, A.E. Finholt, The preparation of sodium borohydride by the high temperature reaction of sodium hydride with borate esters, J. Am. Chem. Soc. 75 (1) (1953) 205–209, https://doi.org/10.1021/ja01097a054

[83] B. Richter, D.B. Ravnsbæk, N. Tumanov, Y. Filinchuk, T.R. Jensen, Manganese borohydride; synthesis and characterization, Dalton Trans. 44 (9) (2015) 3988–3996, https://doi.org/10.1039/C4DT03501A

[84] D.B. Ravnsbæk, E.A. Nickels, R. Černý, C.H. Olesen, W.I.F. David, P.P. Edwards, Y. Filinchuk, T.R. Jensen, Novel alkali earth borohydride Sr(BH4)2 and borohydride-chloride Sr(BH4)Cl, Inorg. Chem. 52 (19) (2013) 10877–10885, https://doi.org/10.1021/ic400862s

[85] H.I. Schlesinger, H.C. Brown, E.K. Hyde, The preparation of other borohydrides by metathetical reactions utilizing the alkali metal borohydrides, J. Am. Chem. Soc. 75 (1) (1953) 209–213, https://doi.org/10.1021/ja01097a055

[86] Y. Yan, H.-W. Li, T. Sato, N. Umeda, K. Miwa, S. Towata, S. Orimo, Dehydriding and rehydriding properties of yttrium borohydride Y(BH4)3 prepared by liquid-phase synthesis, Int. J. Hydrog. Energy 34 (14) (2009) 5732–5736, https://doi.org/10.1016/j.ijhydene.2009.05.097

[87] H.-W. Li, K. Kikuchi, Y. Nakamori, K. Miwa, S. Towata, S. Orimo, Effects of ball milling and additives on dehydriding behaviors of well-crystallized Mg(BH4)2, Scr. Mater. 57 (8) (2007) 679–682, https://doi.org/10.1016/j.scriptamat.2007.06.052

[88] J.E. Olsen, C. Frommen, T.R. Jensen, M.D. Riktor, M.H. Sørby, B.C. Hauback, Structure and thermal properties of composites with re-borohydrides (RE = La, Ce, Pr, Nd, Sm, Eu, Gd, Tb, Er, Yb or Lu) and LiBH4, RSC Adv. 4 (4) (2014) 1570–1582, https://doi.org/10.1039/C3RA44012E

[89] M.B. Ley, M. Paskevicius, P. Schouwink, B. Richter, D.A. Sheppard, C.E. Buckley, T.R. Jensen, Novel solvates M(BH4)3S(CH3)2 and properties of halide-free M (BH4)3 (M = Y or Gd), Dalton Trans. 43 (35) (2014) 13333–13342, https://doi.org/10.1039/C4DT01125B

[90] T.D. Humphries, M.B. Ley, C. Frommen, K.T. Munroe, T.R. Jensen, B.C. Hauback, Crystal structure and in situ decomposition of Eu(BH4)2 and Sm(BH4)2, J. Mater. Chem. A 3 (2) (2015) 691–698, https://doi.org/10.1039/C4TA04080E

[91] C. Frommen, M.H. Sørby, P. Ravindran, P. Vajeeston, H. Fjellvåg, B.C. Hauback, Synthesis, crystal structure, and thermal properties of the first mixed-metal and anion-substituted rare earth borohydride LiCe(BH4)3Cl, J. Phys. Chem. C 115 (47) (2011) 23591–23602, https://doi.org/10.1021/jp205105j

[92] J.E. Olsen, C. Frommen, M.H. Sørby, B.C. Hauback, Crystal structures and properties of solvent-free LiYb(BH4)4−xClx, Yb(BH4)3 and Yb(BH4)2-xClx, RSC Adv. 3 (27) (2013) 10764–10774, https://doi.org/10.1039/C3RA40435H

[93] M.B. Ley, S. Boulineau, R. Janot, Y. Filinchuk, T.R. Jensen, New li ion conductors and solid state hydrogen storage materials: LiM(BH4)3Cl, M = La, Gd, J. Phys. Chem. C. 116 (40) (2012) 21267–21276, https://doi.org/10.1021/jp307762g

[94] E. Grube, C.H. Olesen, D.B. Ravnsbæk, T.R. Jensen, Barium borohydride chlorides: synthesis, crystal structures and thermal properties, Dalton Trans. 45 (19) (2016) 8291–8299, https://doi.org/10.1039/C6DT00772D

[95] W. Wegner, T. Jaroń, W. Grochala, Preparation of a series of lanthanide borohydrides and their thermal decomposition to refractory lanthanide borides, J. Alloy. Compd. 744 (2018) 57–63, https://doi.org/10.1016/j.jallcom.2018.02.020

[96] C. Frommen, M.H. Sørby, M. Heere, T.D. Humphries, J.E. Olsen, B.C. Hauback, Rare earth borohydrides-crystal structures and thermal properties, Energies 10 (12) (2017) 2115, https://doi.org/10.3390/en10122115

[97] W. Wegner, T. Jaroń, W. Grochala, Polymorphism and hydrogen discharge from holmium borohydride, Ho(BH4)3, and KHo(BH4)4, Int. J. Hydrog. Energy 39 (35) (2014) 20024–20030, https://doi.org/10.1016/j.ijhydene.2014.10.013

[98] M.B. Ley, M. Jørgensen, R. Černý, Y. Filinchuk, T.R. Jensen, From M(BH4)3 (M = La, Ce) borohydride frameworks to controllable synthesis of porous hydrides and ion conductors, Inorg. Chem. 55 (19) (2016) 9748–9756, https://doi.org/10.1021/acs.inorgchem.6b01526

[99] M. Heere, S.H.P. GharibDoust, C. Frommen, T.D. Humphries, M.B. Ley, M.H. Sørby, T.R. Jensen, B.C. Hauback, The influence of lih on the rehydrogenation behavior of halide free rare earth (RE) borohydrides (RE = Pr, Er), Phys. Chem. Chem. Phys. 18 (35) (2016) 24387–24395, https://doi.org/10.1039/C6CP04523E

[100] L.H. Jepsen, M.B. Ley, R. Černý, Y.-S. Lee, Y.W. Cho, D. Ravnsbæk, F. Besenbacher, J. Skibsted, T.R. Jensen, Trends in syntheses, structures, and composition of three series of amine rare-earth metal borohydrides, M(BH4)3·nNH3 (M = Y, Gd, and Dy), Inorg. Chem. 54 (15) (2015) 7402–7414, https://doi.org/10.1021/acs.inorgchem.5b00951

[101] J.B. Grinderslev, M.B. Ley, Y.-S. Lee, L.H. Jepsen, M. Jørgensen, Y.W. Cho, J. Skibsted, T.R. Jensen, Ammine lanthanum and cerium borohydrides, M (BH4)3·NH3; trends in synthesis, structures, and thermal properties, Inorg. Chem. 59 (11) (2020) 7768–7778, https://doi.org/10.1021/acs.inorgchem.0c00817

[102] N.A. Tumanov, D.A. Safin, B. Richter, Z. Łodziana, T.R. Jensen, Y. Garcia, Y. Filinchuk, Challenges in the synthetic routes to Mn(BH4)2: insight into intermediate compounds, Dalton Trans. 44 (14) (2015) 6571–6580, https://doi.org/10.1039/C4DT03807J

[103] S. Payandeh GharibDoust, M. Brighi, Y. Sadikin, D.B. Ravnsbæk, R. Černý, J. Skibsted, T.R. Jensen, Synthesis, structure, and Li-Ion conductivity of LiLa (BH4)3X, X = Cl, Br, I, J. Phys. Chem. C 121 (35) (2017) 19010–19021, https://doi.org/10.1021/acs.jpcc.7b04905

[104] S.P. GharibDoust, M. Heere, M.H. Sørby, M.B. Ley, D.B. Ravnsbæk, B.C. Hauback, R. Černý, T.R. Jensen, Synthesis, structure and properties of new bimetallic sodium and potassium lanthanum borohydrides, Dalton Trans. 45 (47) (2016) 19002–19011, https://doi.org/10.1039/C6DT03671F

[105] K.T. Møller, M. Jørgensen, A.S. Fogh, T.R. Jensen, Perovskite alkali metal samarium borohydrides: crystal structures and thermal decomposition, Dalton Trans. 46 (35) (2017) 11905–11912, https://doi.org/10.1039/C7DT02405C

[106] K.T. Møller, M.B. Ley, P. Schouwink, R. Černý, T.R. Jensen, Synthesis and thermal stability of perovskite alkali metal strontium borohydrides, Dalton Trans. 45 (2) (2015) 831–840, https://doi.org/10.1039/C5DT03590B

[107] E.; Roedern, Y.-S.; B. Lee, M.; Ley, K.; Park, Y.; Whan Cho, J.; Skibsted, T.R. Jensen, Solid State synthesis, structural characterization and ionic conductivity of bimetallic alkali-metal yttrium borohydrides MY(BH4)4 (M = Li and Na), J. Mater. Chem. A 4 (22) (2016) 8793–8802, https://doi.org/10.1039/C6TA02761J

[108] K. Chłopek, C. Frommen, A. Léon, O. Zabara, M. Fichtner, Synthesis and properties of magnesium tetrahydroborate, Mg(BH4)2, J. Mater. Chem. 17 (33) (2007) 3496–3503, https://doi.org/10.1039/B702723K

[109] M. Sharma, E. Didelot, A. Spyratou, L.M. Lawson Daku, R. Černý, H. Hagemann, Halide free M(BH4)2 (M = Sr, Ba, and Eu) synthesis, structure, and decomposition, Inorg. Chem. 55 (14) (2016) 7090–7097, https://doi.org/10.1021/acs.inorgchem.6b00931

[110] A.V. Safronov, S.S. Jalisatgi, M.F. Hawthorne, Novel convenient synthesis of 10B-enriched sodium borohydride, Inorg. Chem. 55 (11) (2016) 5116–5117, https://doi.org/10.1021/acs.inorgchem.6b01002

[111] B. Richter, J.B. Grinderslev, K.T. Møller, M. Paskevicius, T.R. Jensen, From metal hydrides to metal borohydrides, Inorg. Chem. 57 (17) (2018) 10768–10780, https://doi.org/10.1021/acs.inorgchem.8b01398

[112] P. Zanella, L. Crociani, N. Masciocchi, G. Giunchi, Facile high-yield synthesis of pure, crystalline Mg(BH4)2, Inorg. Chem. 46 (22) (2007) 9039–9041, https://doi.org/10.1021/ic701436c

[113] T. Jaroń, W. Wegner, K.J. Fijałkowski, P.J. Leszczyński, W. Grochala, Facile formation of thermodynamically unstable novel borohydride materials by a wet

chemistry route, Chem. Eur. J. 21 (15) (2015) 5689–5692, https://doi.org/10. 1002/chem.201404968

[114] T. Jaroń, P.A. Orłowski, W. Wegner, K.J. Fijałkowski, P.J. Leszczyński, W. Grochala, Hydrogen storage materials: room-temperature wet-chemistry approach toward mixed-metal borohydrides, Angew. Chem. Int. Ed. 54 (4) (2015) 1236–1239, https://doi.org/10.1002/anie.201408456

[115] F. Yuan, Q. Gu, X. Chen, Y. Tan, Y. Guo, X. Yu, Complex ammine titanium(iii) borohydrides as advanced solid hydrogen-storage materials with favorable dehydrogenation properties, Chem. Mater. 24 (17) (2012) 3370–3379, https:// doi.org/10.1021/cm301387d

[116] Z. Tang, F. Yuan, Q. Gu, Y. Tan, X. Chen, C.M. Jensen, X. Yu, Scandium and vanadium borohydride ammoniates: enhanced dehydrogenation behavior upon coordinative expansion and establishment of H$^{δ+}$···$^{-δ}$H interactions, Acta Mater. 61 (8) (2013) 3110–3119, https://doi.org/10.1016/j.actamat.2013.02.002

[117] J. Huot, F. Cuevas, S. Deledda, K. Edalati, Y. Filinchuk, T. Grosdidier, B.C. Hauback, M. Heere, T.R. Jensen, M. Latroche, S. Sartori, Mechanochemistry of metal hydrides: recent advances, Materials 12 (17) (2019) 2778, https://doi.org/10.3390/ ma12172778

[118] J. Huot, D.B. Ravnsbæk, J. Zhang, F. Cuevas, M. Latroche, T.R. Jensen, Mechanochemical synthesis of hydrogen storage materials, Prog. Mater. Sci. 58 (1) (2013) 30–75, https://doi.org/10.1016/j.pmatsci.2012.07.001

[119] J.B. Grinderslev, T.R. Jensen, Trends in the series of ammine rare-earth-metal borohydrides: relating structural and thermal properties, Inorg. Chem. 60 (4) (2021) 2573–2589, https://doi.org/10.1021/acs.inorgchem.0c03464

[120] E. Roedern, T.R. Jensen, Ammine-stabilized transition-metal borohydrides of iron, cobalt, and chromium: synthesis and characterization, Inorg. Chem. 54 (21) (2015) 10477–10482, https://doi.org/10.1021/acs.inorgchem.5b01959

[121] F. Yuan, X. Chen, Q. Gu, Z. Tang, X. Yu, Synthesis of ammine dual-metal (V, Mg) borohydrides with enhanced dehydrogenation properties, Int. J. Hydrog. Energy 38 (13) (2013) 5322–5329, https://doi.org/10.1016/j.ijhydene.2013.02.039

[122] S. Aldridge, A.J. Blake, A.J. Downs, R.O. Gould, S. Parsons, C.R. Pulham, Some tetrahydroborate derivatives of aluminium: crystal structures of dimethylaluminium tetrahydroborate and the α and β phases of aluminium tris(tetrahydroborate) at low temperature, J. Chem. Soc. Dalton Trans. 6 (1997) 1007–1012, https://doi.org/10.1039/A607843E

[123] C.J. Dain, A.J. Downs, M.J. Goode, D.G. Evans, K.T. Nicholls, D.W.H. Rankin, H.E. Robertson, Molecular structure of gaseous titanium tris(tetrahydroborate), Ti(BH$_4$)$_3$: experimental determination by electron diffraction and molecular orbital analysis of some Ti(BH$_4$)$_3$ derivatives, J. Chem. Soc. Dalton Trans. 4 (1991) 967–977, https://doi.org/10.1039/DT9910000967

[124] L.H. Rude, M. Corno, P. Ugliengo, M. Baricco, Y.-S. Lee, Y.W. Cho, F. Besenbacher, J. Overgaard, T.R. Jensen, Synthesis and structural investigation of Zr(BH$_4$)$_4$, J. Phys. Chem. C 116 (38) (2012) 20239–20245, https://doi.org/10.1021/jp306665a

[125] R.W. Broach, I.S. Chuang, T.J. Marks, J.M. Williams, Metrical characterization of tridentate tetrahydroborate ligation to a transition-metal ion. structure and bonding in Hf(BH$_4$)$_4$ by single-crystal neutron diffraction, Inorg. Chem. 22 (7) (1983) 1081–1084, https://doi.org/10.1021/ic00149a015

[126] M. Heere, O. Zavorotynska, S. Deledda, M.H. Sørby, D. Book, T. Steriotis, B.C. Hauback, Effect of additives, ball milling and isotopic exchange in porous magnesium borohydride, RSC Adv. 8 (49) (2018) 27645–27653, https://doi.org/ 10.1039/C8RA05146A

[127] O. Zavorotynska, A. El-Kharbachi, S. Deledda, B.C. Hauback, Recent progress in magnesium borohydride Mg(BH$_4$)$_2$: fundamentals and applications for energy storage, Int. J. Hydrog. Energy 41 (32) (2016) 14387–14403, https://doi.org/10. 1016/j.ijhydene.2016.02.015

[128] C. Pistidda, S. Garroni, F. Dolci, E.G. Bardaji, A. Khandelwal, P. Nolis, M. Dornheim, R. Gosalawit, T. Jensen, Y. Cerenius, S. Surinach, M.D. Baro, W. Lohstroh, M. Fichtner, Synthesis of amorphous Mg(BH$_4$)$_2$ from MgB$_2$ and H$_2$ at room temperature, J. Alloy. Compd. 508 (2010) 212–215, https://doi.org/10. 1016/j.jallcom.2010.07.226

[129] V. Ban, A.V. Soloninin, A.V. Skripov, J. Hadermann, A. Abakumov, Y. Filinchuk, Pressure-collapsed amorphous Mg(BH$_4$)$_2$: an ultradense complex hydride showing a reversible transition to the porous framework, J. Phys. Chem. C 118 (40) (2014) 23402–23408, https://doi.org/10.1021/jp507286m

[130] I. Dovgaliuk, V. Dyadkin, M.V. Donckt, Y. Filinchuk, D. Chernyshov, Non-isothermal kinetics of Kr adsorption by nanoporous γ-Mg(BH$_4$)$_2$ from in situ synchrotron powder diffraction, ACS Appl. Mater. Interfaces 12 (6) (2020) 7710–7716, https://doi.org/10.1021/acsami.9b19239

[131] M. Heere, A.-L. Hansen, S. Payandeh, N. Aslan, G. Gizer, M.H. Sørby, B.C. Hauback, C. Pistidda, M. Dornheim, W. Lohstroh, Dynamics of porous and amorphous magnesium borohydride to understand solid state Mg-ion-conductors, Sci. Rep. 10 (1) (2020) 9080, https://doi.org/10.1038/s41598-020-65857-6

[132] L.H. Jepsen, V. Ban, K.T. Møller, Y.-S. Lee, Y.W. Cho, F. Besenbacher, Y. Filinchuk, J. Skibsted, T.R. Jensen, Synthesis, crystal structure, thermal decomposition, and ^{11}B MAS NMR characterization of Mg(BH$_4$)$_2$(NH$_3$BH$_3$)$_2$, J. Phys. Chem. C 118 (23) (2014) 12141–12153, https://doi.org/10.1021/jp502788j

[133] Y. Yang, Y. Liu, Y. Li, M. Gao, H. Pan, Synthesis and thermal decomposition behaviors of magnesium borohydride ammoniates with controllable composition as hydrogen storage materials, Chem. Asian J. 8 (2) (2013) 476–481, https://doi. org/10.1002/asia.201200970

[134] Z. Zhao-Karger, M. Fichtner, Beyond intercalation chemistry for rechargeable Mg batteries: a short review and perspective, Front. Chem. 6 (2019) 656, https://doi.org/10.3389/fchem.2018.00656

[135] A. El Kharbachi, E.M. Dematteis, K. Shinzato, S.C. Stevenson, L.J. Bannenberg, M. Heere, C. Zlotea, P.Á. Szilágyi, J.-P. Bonnet, W. Grochala, D.H. Gregory,

[136] T. Ichikawa, M. Baricco, B.C. Hauback, Metal hydrides and related materials. Energy carriers for novel hydrogen and electrochemical storage, J. Phys. Chem. C 124 (14) (2020) 7599–7607, https://doi.org/10.1021/acs.jpcc.0c01806

[136] S. Payandeh, A. Remhof, C. Battaglia, Solid-state magnesium-ion conductors, Magnesium Batteries: Research and Applications, (2019), pp. 60–78, https:// doi.org/10.1039/9781788016407-00060

[137] S.P. GharibDoust, M. Heere, C. Nervi, M.H. Sørby, B.C. Hauback, T.R. Jensen, Synthesis, structure, and polymorphic transitions of praseodymium(iii) and neodymium(iii) borohydride, Pr(BH$_4$)$_3$ and Nd(BH$_4$)$_3$, Dalton Trans. 47 (25) (2018) 8307–8319, https://doi.org/10.1039/C8DT00118A

[138] A. Gigante, S. Payandeh, J.B. Grinderslev, M. Heere, J.P. Embs, T.R. Jensen, T. Burankova, A. Remhof, H. Hagemann, Structural and dynamic studies of Pr (^{11}BH$_4$)$_3$, Int. J. Hydrog. Energy 46 (2021) 32126–32134, https://doi.org/10.1016/ j.ijhydene.2021.06.232

[139] R.D. Shannon, Revised effective ionic radii and systematic studies of interatomic distances in halides and chalcogenides, Acta Crystallogr. A 32 (5) (1976) 751–767, https://doi.org/10.1107/S0567739476001551

[140] P. Schouwink, V. D'Anna, M.B. Ley, L.M. Lawson Daku, B. Richter, T.R. Jensen, H. Hagemann, R. Černý, Bimetallic borohydrides in the system M(BH$_4$)$_2$–KBH$_4$ (M = Mg, Mn): on the structural diversity, J. Phys. Chem. C 116 (20) (2012) 10829–10840, https://doi.org/10.1021/jp212318s

[141] P. Schouwink, H. Hagemann, J.P. Embs, V. D'Anna, R. Černý, Di-hydrogen contact induced lattice instabilities and structural dynamics in complex hydride perovskites, J. Phys. Condens. Matter 27 (26) (2015) 265403, https://doi.org/10. 1088/0953-8984/27/26/265403

[142] H. Wu, W. Zhou, F.E. Pinkerton, M.S. Meyer, G. Srinivas, T. Yildirim, T.J. Udovic, J.J. Rush, A new family of metal borohydride ammonia borane complexes: synthesis, structures, and hydrogen storage properties, J. Mater. Chem. 20 (31) (2010) 6550–6556, https://doi.org/10.1039/C0JM01542C

[143] T. He, H. Wu, J. Chen, W. Zhou, G. Wu, Z. Xiong, T. Zhang, P. Chen, Alkali and alkaline-earth metal borohydride hydrazinates: synthesis, structures and dehydrogenation, Phys. Chem. Chem. Phys. 15 (25) (2013) 10487–10493, https:// doi.org/10.1039/C3CP51473K

[144] M. Jørgensen, Y.-S. Lee, M. Bjerring, L.H. Jepsen, Ü. Akbey, Y.W. Cho, T.R. Jensen, Disorder induced polymorphic transitions in the high hydrogen density compound Sr(BH$_4$)$_2$(NH$_3$)$_2$, Dalton Trans. 47 (46) (2018) 16737–16746, https:// doi.org/10.1039/C8DT03654C

[145] I. Dovgaliuk, C.S. Le Duff, K. Robeyns, M. Devillers, Y. Filinchuk, Mild dehydrogenation of ammonia borane complexed with aluminum borohydride, Chem. Mater. 27 (3) (2015) 768–777, https://doi.org/10.1021/cm503601h

[146] J.B. Grinderslev, M.S. Andersson, B.A. Trump, W. Zhou, T.J. Udovic, M. Karlsson, T.R. Jensen, Neutron scattering investigations of the global and local structures of ammine yttrium borohydrides, J. Phys. Chem. C 125 (28) (2021) 15415–15423, https://doi.org/10.1021/acs.jpcc.1c03629

[147] Z. Tang, Y. Tan, Q. Gu, X. Yu, A novel aided-cation strategy to advance the dehydrogenation of calcium borohydride monoammoniate, J. Mater. Chem. 22 (12) (2012) 5312–5318, https://doi.org/10.1039/C2JM14990G

[148] W. Sun, X. Chen, Q. Gu, K.S. Wallwork, Y. Tan, Z. Tang, X. Yu, A new ammine dual-cation (Li, Mg) borohydride: synthesis, structure, and dehydrogenation enhancement, Chem. Eur. J. 18 (22) (2012) 6825–6834, https://doi.org/10.1002/ chem.201102651

[149] K.T. Møller, D. Sheppard, D.B. Ravnsbæk, C.E. Buckley, E. Akiba, H.-W. Li, T.R. Jensen, Complex metal hydrides for hydrogen, thermal and electrochemical energy storage, Energies 10 (10) (2017) 1645, https://doi.org/10.3390/ en10101645

[150] A. Unemoto, M. Matsuo, S. Orimo, Complex hydrides for electrochemical energy storage, Adv. Funct. Mater. 24 (16) (2014) 2267–2279, https://doi.org/10.1002/ adfm.201303147

[151] M. Matsuo, Y. Nakamori, S. Orimo, H. Maekawa, H. Takamura, Lithium superionic conduction in lithium borohydride accompanied by structural transition, Appl. Phys. Lett. 91 (22) (2007) 224103, https://doi.org/10.1063/1.2817934

[152] M.N. Guzik, R. Mohtadi, S. Sartori, Lightweight complex metal hydrides for Li-, Na-, and Mg-based batteries, J. Mater. Res. 34 (6) (2019) 877–904, https://doi. org/10.1557/jmr.2019.82

[153] P.E. de Jongh, D. Blanchard, M. Matsuo, T.J. Udovic, S. Orimo, Complex hydrides as room-temperature solid electrolytes for rechargeable batteries, Appl. Phys. A 122 (3) (2016) 251, https://doi.org/10.1007/s00339-016-9807-2

[154] A. Takano, I. Oikawa, A. Kamegawa, H. Takamura, Enhancement of the lithium-ion conductivity of LiBH$_4$ by hydration, Solid State Ion. 285 (2016) 47–50, https://doi.org/10.1016/j.ssi.2015.06.004

[155] R. Zhang, W. Zhao, Z. Liu, S. Wei, Y. Yan, Y. Chen, Enhanced room temperature ionic conductivity of the LiBH$_4$·1/2NH$_3$–Al$_2$O$_3$ composite, Chem. Commun. 57 (19) (2021) 2380–2383, https://doi.org/10.1039/D0CC07296F

[156] W. Zhao, R. Zhang, H. Li, Y. Zhang, Y. Wang, C. Wu, Y. Yan, Y. Chen, Li-ion conductivity enhancement of LiBH$_4$·xNH$_3$ with in situ formed Li$_2$O nanoparticles, ACS Appl. Mater. Interfaces (2021), https://doi.org/10.1021/acsami.1c06164

[157] S. Das, P. Ngene, P. Norby, T. Vegge, P.E. de Jongh, D. Blanchard, All-solid-state lithium-sulfur battery based on a nanoconfined LiBH$_4$ electrolyte, J. Electrochem. Soc. 163 (9) (2016) A2029–A2034, https://doi.org/10.1149/2. 0771609jes

[158] K. Yoshida, K. Suzuki, J. Kawaji, A. Unemoto, S. Orimo, Complex hydride for composite negative electrode-applicable to bulk-type all-solid-state li-ion battery with wide temperature operation, Solid State Ion. 285 (2016) 96–100, https://doi.org/10.1016/j.ssi.2015.07.013

[159] A. Unemoto, C. Chen, Z. Wang, M. Matsuo, T. Ikeshoji, S. Orimo, Pseudo-binary electrolyte, LiBH$_4$–LiCl, for bulk-type all-solid-state lithium-sulfur battery,

Nanotechnology 26 (25) (2015) 254001, https://doi.org/10.1088/0957-4484/26/25/254001

[160] J. Nguyen, B. Fleutot, R. Janot, Investigation of the stability of metal borohydrides-based compounds LiM(BH$_4$)$_3$Cl (M=La, Ce, Gd) as solid electrolytes for Li-S batteries, Solid State Ion. 315 (2018) 26–32, https://doi.org/10.1016/j.ssi.2017.11.033

[161] S. Higashi, K. Miwa, M. Aoki, K. Takechi, A novel inorganic solid state ion conductor for rechargeable mg batteries, Chem. Commun. 50 (2014) 1320–1322, https://doi.org/10.1039/c3cc47097k

[162] R. Le Ruyet, B. Fleutot, R. Berthelot, Y. Benabed, G. Hautier, Y. Filinchuk, R. Janot, Mg$_3$(BH$_4$)$_4$(NH$_2$)$_2$ as inorganic solid electrolyte with high Mg^{2+} ionic conductivity, ACS Appl. Energy Mater. 3 (2020) 6093–6097, https://doi.org/10.1021/acsaem.0c00980

[163] R. Le Ruyet, R. Berthelot, E. Salager, P. Florian, B. Fleutot, R. Janot, Investigation of Mg(BH$_4$)(NH$_2$)-based composite materials with enhanced Mg^{2+} ionic conductivity, J. Phys. Chem. C 123 (17) (2019) 10756–10763, https://doi.org/10.1021/acs.jpcc.9b00616

[164] T. Burankova, E. Roedern, A.E. Maniadaki, H. Hagemann, D. Rentsch, Z. Lodziana, C. Battaglia, A. Remhof, J.P. Embs, Dynamics of the coordination complexes in a solid-state Mg electrolyte, J. Phys. Chem. Lett. 9 (2018) 6450–6455, https://doi.org/10.1021/acs.jpclett.8b02965

[165] D. Aurbach, R. Skaletsky, Y. Gofer, The electrochemical behavior of calcium electrodes in a few organic electrolytes, J. Electrochem. Soc. 138 (12) (1991) 3536–3545, https://doi.org/10.1149/1.2085455

[166] A. Ponrouch, C. Frontera, F. Bardé, M.R. Palacín, Towards a calcium-based rechargeable battery, Nat. Mater. 15 (2) (2016) 169–172, https://doi.org/10.1038/nmat4462

[167] D. Wang, X. Gao, Y. Chen, L. Jin, C. Kuss, P.G. Bruce, Plating and stripping calcium in an organic electrolyte, Nat. Mater. 17 (1) (2018) 16–20, https://doi.org/10.1038/nmat5036

[168] K. Ta, R. Zhang, M. Shin, R.T. Rooney, E.K. Neumann, A.A. Gewirth, Understanding Ca electrodeposition and speciation processes in nonaqueous electrolytes for next-generation Ca-Ion batteries, ACS Appl. Mater. Interfaces 11 (24) (2019) 21536–21542, https://doi.org/10.1021/acsami.9b04926

[169] Y. Jie, Y. Tan, L. Li, Y. Han, S. Xu, Z. Zhao, R. Cao, X. Ren, F. Huang, Z. Lei, G. Tao, G. Zhang, S. Jiao, Electrolyte solvation manipulation enables unprecedented room-temperature calcium-metal batteries, Angew. Chem. Int. Ed. 59 (31) (2020) 12689–12693, https://doi.org/10.1002/anie.202002274

[170] K. Kisu, S. Kim, T. Shinohara, K. Zhao, A. Züttel, S. Orimo, Monocarborane cluster as a stable fluorine-free calcium battery electrolyte, Sci. Rep. 11 (1) (2021) 7563, https://doi.org/10.1038/s41598-021-86938-0

[171] L. Silvi, Z. Zhao-Karger, E. Röhm, M. Fichtner, W. Petry, W. Lohstroh, A quasielastic and inelastic neutron scattering study of the alkaline and alkaline-earth borohydrides LiBH$_4$ and Mg(BH$_4$)$_2$ and the mixture LiBH$_4$ + Mg(BH$_4$)$_2$, Phys. Chem. Chem. Phys. 21 (2) (2019) 718–728, https://doi.org/10.1039/C8CP04316G

[172] L. Silvi, E. Röhm, M. Fichtner, W. Petry, W. Lohstroh, Hydrogen dynamics in β-Mg(BH$_4$)$_2$ on the picosecond timescale, Phys. Chem. Chem. Phys. 18 (21) (2016) 14323–14332, https://doi.org/10.1039/C6CP00995F

[173] M. Dimitrievska, L. White, W. Zhou, V. Stavila, L. E. Klebanoff, T. J. Udovic, Structure-dependent vibrational dynamics of Mg(BH$_4$)$_2$ polymorphs probed with neutron vibrational spectroscopy and first-principles calculations, Phys. Chem. Chem. Phys. 18 (36) (2016) 25546–25552, https://doi.org/10.1039/C6CP04469G

[174] W. Lohstroh, M. Heere, Structure and dynamics of borohydrides studied by neutron scattering techniques: a review, J. Phys. Soc. Jpn. 89 (5) (2020) 051011, https://doi.org/10.7566/JPSJ.89.051011

[175] J. Lefevr, L. Cervini, J.M. Griffin, D. Blanchard, Lithium conductivity and ions dynamics in LiBH$_4$/SiO$_2$ solid electrolytes studied by solid-state nmr and quasielastic neutron scattering and applied in lithium–sulfur batteries, J. Phys. Chem. C 122 (27) (2018) 15264–15275, https://doi.org/10.1021/acs.jpcc.8b01507

[176] R. Zettl, M. Gombotz, D. Clarkson, S.G. Greenbaum, P. Ngene, P.E. de Jongh, H.M.R. Wilkening, Li-Ion diffusion in nanoconfined LiBH$_4$-LiI/Al$_2$O$_3$: from 2D bulk transport to 3D long-range interfacial dynamics, ACS Appl. Mater. Interfaces 12 (34) (2020) 38570–38583, https://doi.org/10.1021/acsami.0c10361

[177] J.A. Santos, P. Simon, A.R. Bernot, C. Babasi, P.A. Ward, S.-J. Hwang, R. Zidan, J.A. Teprovich, Synergistic effect of nanoionic destabilization and partial dehydrogenation for enhanced ionic conductivity in MBH$_4$-C$_{60}$ (M = Li$^+$, Na$^+$) nanocomposites, J. Solid State Electrochem 25 (4) (2021) 1441–1452, https://doi.org/10.1007/s10008-021-04918-w

[178] V. Gulino, L. Barberis, P. Ngene, M. Baricco, P.E. de Jongh, Enhancing Li-Ion conductivity in LiBH$_4$-based solid electrolytes by adding various nanosized oxides, ACS Appl. Energy Mater. 3 (5) (2020) 4941–4948, https://doi.org/10.1021/acsaem.9b02268

[179] M.V. Solovev, O.V. Chashchikhin, P.V. Dorovatovskii, V.N. Khrustalev, A.S. Zyubin, T.S. Zyubina, O.V. Kravchenko, A.A. Zaytsev, Yu.A. Dobrovolsky, Hydrolysis of Mg(BH$_4$)$_2$ and its coordination compounds as a way to obtain hydrogen, J. Power Sources 377 (2018) 93–102, https://doi.org/10.1016/j.jpowsour.2017.11.090

[180] S. Filippov, J.B. Grinderslev, M.S. Andersson, J. Armstrong, M. Karlsson, T.R. Jensen, J. Klarbring, S.I. Simak, U. Häussermann, Analysis of dihydrogen bonding in ammonium borohydride, J. Phys. Chem. C 123 (47) (2019) 28631–28639, https://doi.org/10.1021/acs.jpcc.9b08968

[181] M.S. Andersson, J.B. Grinderslev, T.R. Jensen, V. García-Sakai, U. Häussermann, T.J. Udovic, M. Karlsson, Interplay of NH$_4^+$ and BH$_4^-$ reorientational dynamics in NH$_4$BH$_4$, Phys. Rev. Mater. 4 (8) (2020) 085002, https://doi.org/10.1103/PhysRevMaterials.4.085002

[182] S. Shionoya, W.M. Yen, Phosphor research society (Japon), Phosphor Handbook, CRC Press, Boca Raton; Boston; London, 1999.

[183] E. Snider, N. Dasenbrock-Gammon, R. McBride, M. Debessai, H. Vindana, K. Vencatasamy, K.V. Lawler, A. Salamat, R.P. Dias, Room-temperature superconductivity in a carbonaceous sulfur hydride, Nature 586 (7829) (2020) 373–377, https://doi.org/10.1038/s41586-020-2801-z

[184] M. Somayazulu, M. Ahart, A.K. Mishra, Z.M. Geballe, M. Baldini, Y. Meng, V.V. Struzhkin, R.J. Hemley, Evidence for superconductivity above 260 K in lanthanum superhydride at megabar pressures, Phys. Rev. Lett. 122 (2) (2019) 027001, https://doi.org/10.1103/PhysRevLett.122.027001

[185] A.P. Drozdov, M.I. Eremets, I.A. Troyan, V. Ksenofontov, S.I. Shylin, Conventional superconductivity at 203 kelvin at high pressures in the sulfur hydride system, Nature 525 (7567) (2015) 73–76, https://doi.org/10.1038/nature14964

[186] A.P. Drozdov, P.P. Kong, V.S. Minkov, S.P. Besedin, M.A. Kuzovnikov, S. Mozaffari, L. Balicas, F.F. Balakirev, D.E. Graf, V.B. Prakapenka, E. Greenberg, D.A. Knyazev, M. Tkacz, M.I. Eremets, Superconductivity at 250 K in lanthanum hydride under high pressures, Nature 569 (7757) (2019) 528–531, https://doi.org/10.1038/s41586-019-1201-8

[187] S. Di Cataldo, C. Heil, W. von der Linden, L. Boeri, LaBH$_8$: towards high-tc low-pressure superconductivity in ternary superhydrides, Phys. Rev. B 104 (2) (2021) L020511, https://doi.org/10.1103/PhysRevB.104.L020511

[188] I. Dovgaliuk, H. Hagemann, T. Leyssens, M. Devillers, Y. Filinchuk, CO$_2$-promoted hydrolysis of KBH$_4$ for efficient hydrogen co-generation, Int. J. Hydrog. Energy 39 (34) (2014) 19603–19608, https://doi.org/10.1016/j.ijhydene.2014.09.068

[189] L. Lombardo, Y. Ko, K. Zhao, H. Yang, A. Züttel, Direct CO$_2$ capture and reduction to high-end chemicals with tetraalkylammonium borohydrides, Angew. Chem. 133 (17) (2021) 9666–9675, https://doi.org/10.1002/ange.202100447

[190] T. Wartik, R.K. Pearson, A new type of substituted borohydride, J. Am. Chem. Soc. 77 (4) (1955) 1075, https://doi.org/10.1021/ja01609a107

[191] J.G. Burr, W.G. Brown, H.E. Heller, The reduction of carbon dioxide to formic acid1, J. Am. Chem. Soc. 72 (6) (1950) 2560–2562, https://doi.org/10.1021/ja01162a061

[192] T. Wartik, R.K. Pearson, Reactions of carbon dioxide with sodium and lithium borohydrides, J. Inorg. Nucl. Chem. 7 (4) (1958) 404–411, https://doi.org/10.1016/0022-1902(58)80250-X

[193] I. Knopf, C.C. Cummins, Revisiting CO$_2$ reduction with NaBH$_4$ under aprotic conditions: synthesis and characterization of sodium triformatoborohydride, Organometallics 34 (9) (2015) 1601–1603, https://doi.org/10.1021/acs.organomet.5b00190

[194] K.A. Grice, M.C. Groenenboom, J.D.A. Manuel, M.A. Sovereign, J.A. Keith, Examining the selectivity of borohydride for carbon dioxide and bicarbonate reduction in protic conditions, Fuel 150 (2015) 139–145, https://doi.org/10.1016/j.fuel.2015.02.007

[195] Y. Zhao, Z. Zhang, X. Qian, Y. Han, Properties of carbon dioxide absorption and reduction by sodium borohydride under atmospheric pressure, Fuel 142 (2015) 1–8, https://doi.org/10.1016/j.fuel.2014.10.070

[196] I.N. Pulidindi, B.B. Kimchi, A. Gedanken, Selective chemical reduction of carbon dioxide to formate using microwave irradiation, J. CO2 Util. 7 (2014) 19–22, https://doi.org/10.1016/j.jcou.2014.06.002

[197] C. Fletcher, Y. Jiang, R. Amal, Production of formic acid from CO$_2$ reduction by means of potassium borohydride at ambient conditions, Chem. Eng. Sci. 137 (2015) 301–307, https://doi.org/10.1016/j.ces.2015.06.040

[198] C.V. Picasso, D.A. Safin, I. Dovgaliuk, F. Devred, D. Debecker, H.-W. Li, J. Proost, Y. Filinchuk, Reduction of CO$_2$ with KBH$_4$ in solvent-free conditions, Int. J. Hydrog. Energy 41 (32) (2016) 14377–14386, https://doi.org/10.1016/j.ijhydene.2016.04.052

[199] W. Zhu, J. Zhao, L. Wang, Y.-L. Teng, B.-X. Dong, Mechanochemical reactions of alkali borohydride with CO$_2$ under ambient temperature, J. Solid State Chem. 277 (2019) 828–832, https://doi.org/10.1016/j.jssc.2019.07.037

[200] J.G. Vitillo, E. Groppo, E.G. Bardají, M. Baricco, S. Bordiga, Fast carbon dioxide recycling by reaction with γ-Mg(BH$_4$)$_2$, Phys. Chem. Chem. Phys. 16 (41) (2014) 22482–22486, https://doi.org/10.1039/C4CP03300K

[201] A.F. Baye, M.W. Abebe, R. Appiah-Ntiamoah, H. Kim, Engineered iron-carbon-cobalt (Fe$_3$O$_4$@C-Co) core-shell composite with synergistic catalytic properties towards hydrogen generation via NaBH$_4$ hydrolysis, J. Colloid Interface Sci. 543 (2019) 273–284, https://doi.org/10.1016/j.jcis.2019.02.065

[202] S. Garroni, C. Pistidda, M. Brunelli, G.B.M. Vaughan, S. Suriñach, M.D. Baró, Hydrogen desorption mechanism of 2NaBH$_4$+MgH$_2$ composite prepared by high-energy ball Milling, Scr. Mater. 60 (12) (2009) 1129–1132, https://doi.org/10.1016/j.scriptamat.2009.02.059

[203] F. Karimi, P.K. Pranzas, C. Pistidda, J. A. Puszkiel, C. Milanese, U. Vainio, M. Paskevicius, T. Emmler, A. Santoru, R. Utke, M. Tolkiehn, C. B. Minella, A.-L. Chaudhary, S. Boerries, C. E. Buckley, S. Enzo, A. Schreyer, T. Klassen, M. Dornheim, Structural and kinetic investigation of the hydride composite Ca(BH$_4$)$_2$ + MgH$_2$ system doped with NbF$_5$ for solid-state hydrogen storage, Phys. Chem. Chem. Phys. 17 (41) (2015) 27328–27342, https://doi.org/10.1039/C5CP03557K

[204] G. Barkhordarian, T.R. Jensen, S. Doppiu, U. Bösenberg, A. Borgschulte, R. Gremaud, Y. Cerenius, M. Dornheim, T. Klassen, R. Bormann, Formation of Ca(BH$_4$)$_2$ from hydrogenation of CaH$_2$+MgB$_2$ composite, J. Phys. Chem. C 112 (7) (2008) 2743–2749, https://doi.org/10.1021/jp076325k

[205] B.R.S. Hansen, D. B. Ravnsbæk, J. Skibsted, T. R. Jensen, Hydrogen reversibility of LiBH$_4$–MgH$_2$ –Al composites, Phys. Chem. Chem. Phys. 16 (19) (2014) 8970–8980, https://doi.org/10.1039/C4CP00651H

[206] B.R.S. Hansen, D.B. Ravnsbæk, D. Reed, D. Book, C. Gundlach, J. Skibsted, T.R. Jensen, Hydrogen storage capacity loss in a LiBH$_4$–Al composite, J. Phys. Chem. C 117 (15) (2013) 7423–7432, https://doi.org/10.1021/jp312480h

[207] K.T. Møller, A.S. Fogh, M. Paskevicius, J. Skibsted, T. R. Jensen, Metal borohydride formation from aluminium boride and metal hydrides, Phys. Chem. Chem. Phys. 18 (39) (2016) 27545–27553, https://doi.org/10.1039/C6CP05391B

[208] U.B. Demirci, O. Akdim, J. Andrieux, J. Hannauer, R. Chamoun, P. Miele, Sodium borohydride hydrolysis as hydrogen generator: issues, state of the art and applicability upstream from a fuel cell, Fuel Cells 10 (3) (2010) 335–350, https://doi.org/10.1002/fuce.200800171

[209] F. Lu, Y. Pang, M. Zhu, F. Han, J. Yang, F. Fang, D. Sun, S. Zheng, C. Wang, A high-performance Li–B–H electrolyte for all-solid-state li batteries, Adv. Funct. Mater. 29 (15) (2019) 1809219, https://doi.org/10.1002/adfm.201809219

[210] Y.S. Choi, Y.-S. Lee, K.H. Oh, Y.W. Cho, Interface-enhanced li ion conduction in a LiBH$_4$–SiO$_2$ solid electrolyte, Phys. Chem. Chem. Phys. 18 (32) (2016) 22540–22547, https://doi.org/10.1039/C6CP03563A

[211] Suwarno, P. Ngene, A. Nale, T.M. Eggenhuisen, M. Oschatz, J.P. Embs, A. Remhof, P.E. de Jongh, Confinement effects for lithium borohydride: comparing silica and carbon scaffolds, J. Phys. Chem. C Nanomater. Interfaces 121 (8) (2017) 4197–4205, https://doi.org/10.1021/acs.jpcc.6b13094

[212] V. Gulino, M. Brighi, F. Murgia, P. Ngene, P. de Jongh, R. Černý, M. Baricco, Room-temperature solid-state lithium-ion battery using a LiBH$_4$–MgO composite electrolyte, ACS Appl. Energy Mater. 4 (2021) 1228–1236, https://doi.org/10.1021/acsaem.0c02525

[213] W.D. Richards, L.J. Miara, Y. Wang, J.C. Kim, G. Ceder, Interface stability in solid-state batteries, Chem. Mater. 28 (1) (2016) 266–273, https://doi.org/10.1021/acs.chemmater.5b04082

[214] Z. Lu, F. Ciucci, Metal borohydrides as electrolytes for solid-state Li, Na, Mg, and Ca batteries: a first-principles study, Chem. Mater. 29 (21) (2017) 9308–9319, https://doi.org/10.1021/acs.chemmater.7b03284

[215] R. Asakura, L. Duchêne, R.-S. Kühnel, A. Remhof, H. Hagemann, C. Battaglia, Electrochemical oxidative stability of hydroborate-based solid-state electrolytes, ACS Appl. Energy Mater. 2 (9) (2019) 6924–6930, https://doi.org/10.1021/acsaem.9b01487

[216] J. Kasemchainan, S. Zekoll, D. Spencer Jolly, Z. Ning, G.O. Hartley, J. Marrow, P.G. Bruce, Critical stripping current leads to dendrite formation on plating in lithium anode solid electrolyte cells, Nat. Mater. 18 (10) (2019) 1105–1111, https://doi.org/10.1038/s41563-019-0438-9

[217] A. Unemoto, T. Ikeshoji, S. Yasaku, M. Matsuo, V. Stavila, T.J. Udovic, S. Orimo, Stable interface formation between TiS$_2$ and LiBH$_4$ in bulk-type all-solid-state lithium batteries, Chem. Mater. 27 (15) (2015) 5407–5416, https://doi.org/10.1021/acs.chemmater.5b02110

[218] L.M. Riegger, R. Schlem, J. Sann, W.G. Zeier, J. Janek, Lithium-metal anode instability of the superionic halide solid electrolytes and the implications for solid-state batteries, Angew. Chem. Int. Ed. 60 (12) (2021) 6718–6723, https://doi.org/10.1002/anie.202015238

[219] T. Famprikis, P. Canepa, J.A. Dawson, M.S. Islam, C. Masquelier, Fundamentals of inorganic solid-state electrolytes for batteries, Nat. Mater. 18 (12) (2019) 1278–1291, https://doi.org/10.1038/s41563-019-0431-3

[220] J. Auvergniot, A. Cassel, J.-B. Ledeuil, V. Viallet, V. Seznec, R. Dedryvère, Interface stability of argyrodite Li$_6$PS$_5$Cl toward LiCoO$_2$, LiNi$_{1/3}$Co$_{1/3}$Mn$_{1/3}$O$_2$, and LiMn$_2$O$_4$ in bulk all-solid-state batteries, Chem. Mater. 29 (9) (2017) 3883–3890, https://doi.org/10.1021/acs.chemmater.6b04990

[221] F. Walther, R. Koerver, T. Fuchs, S. Ohno, J. Sann, M. Rohnke, W.G. Zeier, J. Janek, Visualization of the interfacial decomposition of composite cathodes in argyrodite-based all-solid-state batteries using time-of-flight secondary-ion mass spectrometry, Chem. Mater. 31 (10) (2019) 3745–3755, https://doi.org/10.1021/acs.chemmater.9b00770

[222] R. Koerver, I. Aygün, T. Leichtweiß, C. Dietrich, W. Zhang, J.O. Binder, P. Hartmann, W.G. Zeier, J. Janek, Capacity fade in solid-state batteries: interphase formation and chemomechanical processes in Nickel-Rich layered oxide cathodes and lithium thiophosphate solid electrolytes, Chem. Mater. 29 (13) (2017) 5574–5582, https://doi.org/10.1021/acs.chemmater.7b00931

[223] M. Rashad, M. Asif, Y. Wang, Z. He, I. Ahmed, Recent advances in electrolytes and cathode materials for magnesium and hybrid-ion batteries, Energy Storage Mater. 25 (2020) 342–375, https://doi.org/10.1016/j.ensm.2019.10.004

[224] R. Mohtadi, O. Tutusaus, T.S. Arthur, Z. Zhao-Karger, M. Fichtner, The metamorphosis of rechargeable magnesium batteries, Joule 5 (3) (2021) 581–617, https://doi.org/10.1016/j.joule.2020.12.021

[225] R. Černý, M. Brighi, F. Murgia, The crystal chemistry of inorganic hydroborates, Chemistry 2 (4) (2020) 805–826, https://doi.org/10.3390/chemistry2040053

[226] M. Brighi, F. Murgia, R. Černý, Closo-hydroborate sodium salts as an emerging class of room-temperature solid electrolytes, Cell Rep. Phys. Sci. 1 (2020) 100217, https://doi.org/10.1016/j.xcrp.2020.100217

[227] K.T. Møller, T.R. Jensen, E. Akiba, H. Li, Hydrogen - a sustainable energy carrier, Prog. Nat. Sci. Mater. Int. 27 (1) (2017) 34–40, https://doi.org/10.1016/j.pnsc.2016.12.014

[228] M. Hirscher, V.A. Yartys, M. Baricco, J. Bellosta von Colbe, D. Blanchard, R.C. Bowman, D.P. Broom, C.E. Buckley, F. Chang, P. Chen, Y.W. Cho, J.-C. Crivello, F. Cuevas, W.I.F. David, P.E. de Jongh, R.V. Denys, M. Dornheim, M. Felderhoff, Y. Filinchuk, G.E. Froudakis, D.M. Grant, E.MacA. Gray, B.C. Hauback, T. He, T.D. Humphries, T.R. Jensen, S. Kim, Y. Kojima, M. Latroche, H.-W. Li, M.V. Lototskyy, J.W. Makepeace, K.T. Møller, L. Naheed, P. Ngene, D. Noréus, M.M. Nygård, S. Orimo, M. Paskevicius, L. Pasquini, D.B. Ravnsbæk, M. Veronica Sofianos, T.J. Udovic, T. Vegge, G.S. Walker, C.J. Webb, C. Weidenthaler, C. Zlotea, Materials for hydrogen-based energy storage – past, recent progress and future outlook, J. Alloy. Compd. 827 (2020) 153548, https://doi.org/10.1016/j.jallcom.2019.153548

[229] L.J. Bannenberg, M. Heere, H. Benzidi, J. Montero, E.M. Dematteis, S. Suwarno, T. Jaroń, M. Winny, P.A. Orłowski, W. Wegner, A. Starobrat, K.J. Fijałkowski, W. Grochala, Z. Qian, J.-P. Bonnet, I. Nuta, W. Lohstroh, C. Zlotea, O. Mounkachi, F. Cuevas, C. Chatillon, M. Latroche, M. Fichtner, M. Baricco, B.C. Hauback, A. El Kharbachi, Metal (boro-) hydrides for high energy density storage and relevant emerging technologies, Int. J. Hydrog. Energy 45 (2020) 33687–33730, https://doi.org/10.1016/j.ijhydene.2020.08.119